Generalized unitarity and six-dimensional helicity

Zvi Bern, John Joseph Carrasco, Tristan Dennen, Yu-tin Huang, and Harald Ita

Phys. Rev. D **83**, 085022 — Published 21 April 2011

DOI: 10.1103/PhysRevD.83.085022

SU-ITP-10/29 UCLA/10/TEP/107

Generalized Unitarity and Six-Dimensional Helicity

Zvi Bern[a], John Joseph Carrasco[b], Tristan Dennen[a], Yu-tin Huang[a] and Harald Ita[a]

[a] *Department of Physics and Astronomy*
UCLA, Los Angeles, CA 90095-1547, USA

[b] *Department of Physics, Stanford University*
Stanford, CA 94305-4060, USA

We combine the unitarity method with the six-dimensional helicity formalism of Cheung and O'Connell to construct loop-level scattering amplitudes. As a first example, we construct dimensionally regularized QCD one-loop four-point amplitudes. As a nontrivial multiloop example, we confirm that the recently constructed four-loop four-point amplitude of $\mathcal{N} = 4$ super-Yang-Mills theory, including nonplanar contributions, is valid for dimensions $D \leq 6$. We comment on the connection of our approach to the recently discussed Higgs infrared regulator and on dual conformal properties in six dimensions.

PACS numbers: 12.38.-t, 12.38.Bx, 13.87.-a, 14.70.-e

I. INTRODUCTION

Recent years have seen a renaissance in the study of scattering amplitudes. This has been driven in part by the need for reliable next-to-leading-order QCD calculations for experiments at the Large Hadron Collider. It has also been driven by the realization of profound hidden structures in scattering amplitudes whose full import remains to be unraveled. A key idea for many of the advances has been that new amplitudes should be constructed using only simpler on-shell amplitudes [1, 2], avoiding unphysical gauge-dependent quantities in intermediate steps. The on-shell viewpoint has revealed a number of remarkable structures in gauge theories, including a description of amplitudes in terms of curves in twistor space [3], and a duality between color and kinematics [4]. Maximally supersymmetric planar amplitudes have an even richer structure, for example all-order resummations of planar amplitudes valid at both weak and strong coupling [5, 6], new symmetries [7–9] and a Grassmannian structure [10]. On the practical side, on-shell methods have allowed ever more complex calculations in next-to-leading-order QCD [11], supersymmetric gauge theories [12–15] and supergravity theories to be carried out [16–19].

The unitarity method [1, 12, 20–31] gives a means for constructing complete loop amplitudes directly from on-shell tree amplitudes. These methods are efficient and display a relatively tame growth in complexity with increasing number of external particles or loops, especially when compared to traditional Feynman-diagrammatic approaches. With this approach, it is usually advantageous to simplify the input tree amplitudes as much as possible prior to applying them in loop calculations. A key tool for simplifying massless tree amplitudes strictly in four dimensions has been spinor helicity [32, 33]. However, if we use dimensional regularization or any form of massive regularization, massless four-dimensional spinor helicity techniques are no longer directly applicable within the loops.

In this paper we will describe a unitarity-based approach using the six-dimensional spinor-helicity formalism of Cheung and O'Connell [34] to avoid these limitations. As in four dimensions, the six-dimensional spinor-helicity formalism offers a relatively compact representation of amplitudes, making manifest little-group properties. Here we are concerned with two basic applications: one-loop QCD amplitudes and multiloop scattering amplitudes in $\mathcal{N} = 4$ super-Yang-Mills (sYM) theory. Although related, there are differences in the technical demands of the two cases. In particular, the QCD amplitudes have both ultraviolet and infrared divergences, while the $\mathcal{N} = 4$ amplitudes have only the latter. All these divergences need to be regularized. On the other hand, the supersymmetric theory needs an efficient formalism to organize its spectrum of states, especially at high-loop orders, in much the same way as done in four dimensions using an on-shell superspace [35–38]. As we discuss, both aspects can be addressed using six-dimensional spinor helicity.

In the past, the main bottleneck for carrying out next-to-leading-order QCD calculations. has been the difficulty of evaluating one-loop amplitudes [39]. The unitarity method offers a universal solution to this difficulty that scales well with the number of external legs. Any contributions which can be captured by four-dimensional techniques —

the so called "cut-constructible pieces" — may be computed efficiently using four-dimensional helicity states in the cuts [1, 23, 27, 40]. The remaining rational contributions tend to be the most complex (and time consuming) parts of calculations, though there are a number of techniques for dealing with such pieces. In the bootstrap approach, the rational pieces are constructed by on-shell recursion in four dimensions [40, 41]. Another approach uses D-dimensional generalized unitarity [21, 22, 25, 28, 30, 42]. A six-dimensional unitarity procedure for any one-loop QCD amplitude has been given in ref. [30] using the on-shell procedure of reducing integrals in ref. [26]. A related approach makes use of the relation between massive states in four dimensions and those in extra dimensions to reduce the integrals obtained from unitarity cuts [21, 31]. The six-dimensional helicity approach described here is well suited for either of the latter two approaches for carrying out integral reductions. A convenient means for doing so is by reexpressing the spinors of our six-dimensional approach as four-dimensional spinors and what are effectively mass parameters. This gives expressions similar to those used in Badger's four-dimensional massive approach [31]. We illustrate this using some simple one-loop four-gluon contributions to QCD amplitudes [21].

We will also consider multiloop $\mathcal{N} = 4$ sYM amplitudes. To set this up, we make use of the six-dimensional on-shell superspace constructed by two of the authors and Siegel (DHS) [43]. General constructions of on-shell superspaces have been discussed in ref. [44]. In strictly four dimensions we have a well-developed on-shell superspace [35–38] for tracking contributions from different states in the multiplet. However,as already noted above this leaves open the question of whether contributions are missed by using four-dimensional momenta in the unitarity cuts or in the recent BCFW constructions of planar loop integrands [15, 45]. This is especially important when constructing amplitudes for use in $D > 4$ studies, but even in dimensionally regularized four-dimensional expressions, when divergences are present, there can be nonvanishing contributions from terms that vanish naively in four dimensions. This becomes more important as the loop order or the number of external legs grows, allowing for a greater number of potentially problematic terms. Besides terms with explicit dependence on extra-dimensional momenta, such terms can be formed from antisymmetric combinations momenta which vanish in four dimensions. For example, we know that dimensionally regularized two-loop six-point amplitudes in $\mathcal{N} = 4$ sYM theory have such terms [14]. In theories with fewer supersymmetries, such terms occur with more frequency, and, for example, appear in one-loop QCD amplitudes [21].

To illustrate the supersymmetric formalism, we first describe the three-particle cut of the planar two-loop four-point $\mathcal{N} = 4$ amplitude [46], before turning to the rather nontrivial case of four-loop four-point amplitudes in this theory, including the nonplanar terms. The latter amplitude has recently been computed [47], using mainly four-dimensional techniques. Direct calculations of four-point gluon amplitudes in $\mathcal{N} = 1$ sYM in $D = 10$ dimensions, which upon dimensional reduction gives $\mathcal{N} = 4$ sYM theory, confirm that all terms are captured by calculating directly in four dimensions, through three loops.[1] At four loops, similar $D = 10$ checks have been performed in the planar case, up to a mild assumption that no term has a worse power count than the amplitude [8]. However, in the case of nonplanar contributions, there is no complete check that the expressions built using four-dimensional momenta in the cuts are complete, although a number of strong consistency checks have been performed [47]. In this paper we confirm that the expressions for the amplitudes of ref. [47] are valid for $D \leq 6$, as expected.

The higher-dimensional viewpoint offers a simple way to introduce a gauge-invariant massive regulator. If we do not integrate the loop momenta over the extra-dimensional momenta, but integrate over only a four-dimensional subspace, we obtain a massive infrared regulator, where the masses are effectively the extra-dimensional momenta. This allows us to connect to the massive Higgs regulator recently developed by Alday, Henn, Plefka and Schuster [48], which offers a number of advantages over dimensional regularization for planar $\mathcal{N} = 4$ sYM amplitudes. Although it seems likely that terms proportional to the mass are suppressed as $m \to 0$ [15], such mass terms are important for studies of the Coulomb branch of $\mathcal{N} = 4$ sYM theory. In many cases it is straightforward to convert the previously determined dimensionally regularized massless integrands to massive forms [48]. Nevertheless, one would like a means for obtaining or confirming such integrands directly via unitarity to ensure their reliability or for deriving regulators valid for the nonplanar case. The six-dimensional on-shell superspace approach gives us a convenient means for doing this.

At four points, the integrands of $\mathcal{N} = 4$ sYM integrands do not depend explicitly on the space-time dimension, but only implicitly through Lorentz dot products, as already noted in refs. [8, 16–18, 46, 47, 49] and explicitly confirmed here at four loops. This suggests that the dual conformal properties, which impose strong constraints on the form of the integrands in four dimensions, will impose similar constraints in higher dimensions. In addition, dual conformal invariance can be extended to the massive Higgs-regulated case [48]. These facts suggest that the dual conformal properties of planar $\mathcal{N} = 4$ sYM amplitudes should have extensions away from four dimensions. Motivated by this, we

[1] This property is special to maximal supersymmetry, and we have no expectation that it should hold for other theories.

write down generators for dual conformal transformations in six dimensions and propose transformation properties, which are straightforward to check at four points using the known expressions.

Finally, we also note that with the six-dimensional helicity formalism contributions to amplitudes factorize into products of chiral-conjugate pairs. Since it holds in all cuts which decompose loop amplitudes into sums of products of tree amplitudes, it seems reasonable that it holds at loop level as well. Although this structure is somewhat reminiscent of the recently discovered double-copy structure of gravity-diagram numerators [4, 50], as we shall see, there are a number of significant differences. Nevertheless, it can help simplify calculations.

This paper is organized as follows: In section II we review the six-dimensional helicity formalism, showing the connection to four-dimensional helicity, briefly review the unitarity method in the context of this formalism, and discuss modifications needed for obtaining massive regulators. Then in section III we review BCFW recursion in six dimensions, before describing the chiral-conjugate property. In section IV we turn to our first examples, which are one-loop four-point amplitudes of QCD. In section V we review an on-shell superspace compatible with six-dimensional helicity. We give special care to the three-point amplitude since new variables are needed. We also develop the necessary building blocks for high-loop unitarity cuts using on-shell recursion. Then in section VI we turn to high-loop applications, using the two-loop four-point amplitude as an example to illustrate the methods before turning to higher loops. In section VII we then discuss an extension of dual conformal properties to six dimensions. We give our comments and prospects for future developments in section VIII. We include two appendices, one showing the analytic results of a nontrivial cut of the four-loop four-point amplitude and the other collecting auxiliary variables [34] needed for defining three-point tree amplitudes.

II. SIX-DIMENSIONAL HELICITY

We begin by summarizing Cheung and O'Connell's six-dimensional spinor-helicity formalism [34]. To make the connection to four-dimensional spinor techniques more transparent, we choose to write the six-dimensional spinors in terms of the more conventional four-dimensional ones [43, 44]. This form is particularly well suited for carrying out loop calculations in dimensional regularization, as needed for QCD computations. It also allows us to interpret the extra-dimensional contributions in terms of masses.

A. Spinor helicity

Before we review the six-dimensional helicity formalism, we state our conventions of spinors in four dimensions. We follow ref. [33] and work in a Weyl basis for the spinors such that $p_{\alpha\dot\alpha} = \lambda_{p\alpha}\tilde\lambda_{p\dot\alpha}$. We use the bra-ket notation for the chiral spinors and their contractions,

$$\langle i\,j\rangle = \epsilon^{\alpha\beta}\lambda_{i\,\beta}\lambda_{j\,\alpha}\,, \quad [i\,j] = \epsilon_{\dot\alpha\dot\beta}\tilde\lambda_i^{\dot\beta}\tilde\lambda_j^{\dot\alpha}\,, \quad \text{and} \quad \langle i\,j\rangle\,[j\,i] = 2\,p_i{\cdot}p_j = s_{ij}\,, \tag{2.1}$$

with $\epsilon_{12} = -1$, $\epsilon^{12} = 1$. For further details we refer to the above-mentioned review.[2]

In six dimensions, a vector can be expressed using the spinor representation of SO(5,1),

$$p_{AB} = p_\mu \sigma^\mu_{AB}\,, \qquad\qquad p^{AB} = p_\mu \tilde\sigma^{\mu AB}\,, \tag{2.2}$$

where $\{A, B\cdots\}$ are fundamental representation indices of the covering group, $\mathrm{SU}^*(4)$. Here the σ^μ_{AB} and $\tilde\sigma^{\mu AB}$ are antisymmetric 4×4 matrices which play a role analogous to the Pauli matrices in four dimensions. Further details and explicit forms of the matrices may be found in Appendix A of ref. [34]. The Dirac equation for Weyl spinors in six dimensions can be written as,

$$p_\mu \sigma^\mu_{AB}\lambda_p^{Ba} = 0\,, \qquad\qquad p_\mu \tilde\sigma^{\mu AB}\,\tilde\lambda_{pB\dot a} = 0\,, \tag{2.3}$$

and gives rise to two independent solutions for each of the Weyl spinors, λ^{Ba} and $\tilde\lambda_{B\dot a}$. Each solution is labeled by indices a or $\dot a$, which are spinor indices of the little group SO(4), corresponding to SU(2)×SU(2). We may lower and raise the little group SU(2) indices $a, \dot a$ with the matrices ϵ_{ab} and $\epsilon^{\dot a\dot b}$,

$$\lambda_a = \epsilon_{ab}\lambda^b\,, \qquad\qquad \tilde\lambda^{\dot a} = \epsilon^{\dot a\dot b}\tilde\lambda_{\dot b}\,, \tag{2.4}$$

[2] Ref. [34] differ by a sign in the definitions of four-dimensional spinor angle brackets so that instead $\langle i\,j\rangle\,[j\,i] = -s_{ij}$.

and $\epsilon_{12} = -1$, $\epsilon^{12} = 1$, for this case as well. Spinor inner products are defined by contractions of the SU*(4) indices,

$$\langle i^a | j_{\dot{b}}] = \lambda_i^{Aa} \tilde{\lambda}_{jA\dot{b}} = [j_{\dot{b}} | i^a \rangle \,. \tag{2.5}$$

Other common quantities are spinors contracted with the SU*(4)-invariant Levi-Civita tensor,

$$\begin{aligned} \langle i^a j^b k^c l^d \rangle &\equiv \epsilon_{ABCD} \lambda_i^{Aa} \lambda_j^{Bb} \lambda_k^{Cc} \lambda_l^{Dd} \,, \\ [i_{\dot{a}} j_{\dot{b}} k_{\dot{c}} l_{\dot{d}}] &\equiv \epsilon^{ABCD} \tilde{\lambda}_{iA\dot{a}} \tilde{\lambda}_{jB\dot{b}} \tilde{\lambda}_{kC\dot{c}} \tilde{\lambda}_{lD\dot{d}} \,. \end{aligned} \tag{2.6}$$

The on-shell massless condition can be solved using bosonic six-dimensional chiral spinors in a way similar to the well-known four-dimensional case. The antisymmetry of p_{AB} together with the on-shell condition $p^2 \sim \epsilon^{ABCD} p_{AB} p_{CD} = 0$ gives the bispinor representation,

$$p^{AB} = \lambda^{Aa} \, \epsilon_{ab} \lambda^{Bb} \,, \qquad p_{AB} = \tilde{\lambda}_{A\dot{a}} \, \epsilon^{\dot{a}\dot{b}} \tilde{\lambda}_{B\dot{b}} \,, \qquad \lambda^{Aa} \tilde{\lambda}_{A\dot{a}} = 0 \,. \tag{2.7}$$

One can also express the vector momenta directly in terms of the spinors via,

$$p^\mu = -\frac{1}{4} \langle p^a | \sigma^\mu | p^b \rangle \epsilon_{ab} = -\frac{1}{4} [p_{\dot{a}} | \tilde{\sigma}^\mu | p_{\dot{b}}] \epsilon^{\dot{a}\dot{b}} \,. \tag{2.8}$$

Other useful quantities appearing in amplitudes are spinor strings,

$$\begin{aligned} \langle i^a | \not{p}_1 \not{p}_2 \cdots \not{p}_{2n+1} | j^b \rangle &= (\lambda_i)^{A_1 a} \, (p_1)_{A_1 A_2} \, (p_2)^{A_2 A_3} \cdots (p_{2n+1})_{A_{2n+1} A_{2n+2}} \, (\lambda_j)^{A_{2n+2} b} \,, \\ \langle i^a | \not{p}_1 \not{p}_2 \cdots \not{p}_{2n} | j_{\dot{b}}] &= (\lambda_i)^{A_1 a} \, (p_1)_{A_1 A_2} \, (p_2)^{A_2 A_3} \, \cdots (p_{2n})^{A_{2n} A_{2n+1}} \, (\tilde{\lambda}_j)_{A_{2n+1} \dot{b}} \,. \end{aligned} \tag{2.9}$$

In six dimensions we have four polarization states. Following Cheung and O'Connell, the polarization vectors can be written as [34],

$$\epsilon^\mu_{a\dot{a}}(p,k) = \frac{1}{\sqrt{2}} \langle p_a | \sigma^\mu | k_b \rangle (\langle k_b | p^{\dot{a}}])^{-1} = (\langle p^a | k_{\dot{b}}])^{-1} \frac{1}{\sqrt{2}} [k_{\dot{b}} | \tilde{\sigma}^\mu | p_{\dot{a}}] \,, \tag{2.10}$$

where the a and $\dot{a}$ indices are labels for the four polarization states. As for the four-dimensional case, we have a null reference momentum k to define the states. For each of the Weyl spinors $[i^{\dot{a}} |$ and $\langle j_a |$ the indices a and $\dot{a}$ label two helicity states respectively. The object $(\langle p^a | k_{\dot{b}}])^{-1} = -(\langle p_a | k^{\dot{b}}])/2p \cdot k$ is the inverse matrix of the spinor product $\langle p^a | k_{\dot{b}}]$ with respect to the helicity indices. As for the four-dimensional case, the polarization vectors are transverse, and a redefinition of the reference spinor can be shown to correspond to a gauge transformation.

Given the proliferation of indices, we now summarize the indices that appear. For four-dimensional objects the indices are,

$$\begin{aligned} \text{SL(2,C) fundamental labels:} &\qquad \alpha, \beta, \gamma, \ldots = 1, 2 \,, \quad \text{and} \quad \dot{\alpha}, \dot{\beta}, \dot{\gamma}, \ldots = 1, 2 \,, \\ \text{SO(3,1) vector labels:} &\qquad \mu, \nu, \rho, \ldots = 0, 1, 2, 3 \,, \end{aligned} \tag{2.11}$$

For six-dimensional objects the indices are,

$$\begin{aligned} \text{SU}^*\text{(4) fundamental labels:} &\qquad A, B, C, \ldots = 1, 2, 3, 4 \\ \text{SO(5,1) vector labels:} &\qquad \mu, \nu, \rho, \ldots = 0, 1, 2, \ldots 5 \\ \text{SU(2)}\times\text{SU(2) helicity labels:} &\qquad a, b, c, \ldots = 1, 2 \quad \text{and} \quad \dot{a}, \dot{b}, \dot{c}, \ldots = 1, 2 \,. \end{aligned} \tag{2.12}$$

The six-dimensional spinors will be identifiable because they carry SU(2)×SU(2) little-group helicity indices.

B. Decomposing six-dimensional spinors into four-dimensional ones

For many purposes, it is convenient to express the six-dimensional spinors in terms of the better-known four-dimensional ones [43, 44]. This allows us to define a physical four-dimensional subspace, and identify states polarized within and transverse to it.

Viewed from four dimensions, the six-dimensional massless condition is that of a massive four-dimensional vector,

$$p^2 = {}^{(4)}p^2 - p_4^2 - p_5^2 \equiv {}^{(4)}p^2 - m\tilde{m} = 0\,, \tag{2.13}$$

where ${}^{(4)}p$ denotes a momentum vector keeping only the first four components. The masses are related to the fifth and sixth components of the momentum,

$$m \equiv p_5 - ip_4\,, \qquad \tilde{m} \equiv p_5 + ip_4\,, \tag{2.14}$$

where we have chosen the masses to be complex, since these will be the natural combinations appearing in six-dimensional spinors when decomposed into four-dimensional ones. In general, massive momenta can be expressed in terms of two pairs of four-dimensional spinors, here denoted by $\lambda, \tilde{\lambda}$ and $\mu, \tilde{\mu}$, via,

$${}^{(4)}p_{\alpha\dot{\alpha}} = \lambda_\alpha \tilde{\lambda}_{\dot{\alpha}} + \rho\, \mu_\alpha \tilde{\mu}_{\dot{\alpha}}\,, \tag{2.15}$$

where,

$$\rho = \kappa\tilde{\kappa} = \kappa'\tilde{\kappa}'\,, \quad \kappa \equiv \frac{m}{\langle \lambda\, \mu\rangle}\,, \quad \tilde{\kappa} = \frac{\tilde{m}}{[\mu\, \lambda]}\,, \quad \kappa' \equiv \frac{\tilde{m}}{\langle \lambda\, \mu\rangle}\,, \quad \tilde{\kappa}' = \frac{m}{[\mu\, \lambda]}\,. \tag{2.16}$$

Treating the six-dimensional spinors $\lambda^A{}_a$ and $\tilde{\lambda}_{A\dot{a}}$ as 4×2 matrices, the six-dimensional massless spinors can then be expressed in terms of the above massless four-dimensional spinors via,

$$\lambda^A{}_a = \begin{pmatrix} -\kappa\mu_\alpha & \lambda_\alpha \\ \tilde{\lambda}^{\dot{\alpha}} & \tilde{\kappa}\tilde{\mu}^{\dot{\alpha}} \end{pmatrix}\,, \qquad \tilde{\lambda}_{A\dot{a}} = \begin{pmatrix} \kappa'\mu^\alpha & \lambda^\alpha \\ -\tilde{\lambda}_{\dot{\alpha}} & \tilde{\kappa}'\tilde{\mu}_{\dot{\alpha}} \end{pmatrix}\,. \tag{2.17}$$

The two columns in $\lambda^A{}_a$ and $\tilde{\lambda}_{A\dot{a}}$ correspond to the little-group index a and $\dot{a}$ taking value 1 or 2 respectively. This particular embedding of the four-dimensional spinors is constrained by the explicit form of the σ^μ_{AB} matrices used here. Using this, we can express the six-dimensional momenta in terms of the antisymmetric matrices,

$$\begin{aligned} p^{AB} &= \begin{pmatrix} -m\,\epsilon_{\alpha\beta} & \lambda_\alpha \tilde{\lambda}^{\dot{\beta}} + \rho\, \mu_\alpha \tilde{\mu}^{\dot{\beta}} \\ -\tilde{\lambda}^{\dot{\alpha}}\lambda_\beta - \rho\, \tilde{\mu}^{\dot{\alpha}}\mu_\beta & \tilde{m}\,\epsilon^{\dot{\alpha}\dot{\beta}} \end{pmatrix}\,, \\ p_{AB} &= \begin{pmatrix} \tilde{m}\,\epsilon^{\alpha\beta} & \lambda^\alpha \tilde{\lambda}_{\dot{\beta}} + \rho\, \mu^\alpha \tilde{\mu}_{\dot{\beta}} \\ -\tilde{\lambda}_{\dot{\alpha}}\lambda^\beta - \rho\, \tilde{\mu}_{\dot{\alpha}}\mu^\beta & -m\,\epsilon_{\dot{\alpha}\dot{\beta}} \end{pmatrix}\,, \end{aligned} \tag{2.18}$$

where AB are the antisymmetric SU*(4) indices.

If we choose momenta which lie in the four-dimensional subspace $p^{4,5} = 0$, the spinors simplify to,

$$\lambda^A{}_a = \begin{pmatrix} 0 & \lambda_\alpha \\ \tilde{\lambda}^{\dot{\alpha}} & 0 \end{pmatrix}\,, \qquad \tilde{\lambda}_{A\dot{a}} = \begin{pmatrix} 0 & \lambda^\alpha \\ -\tilde{\lambda}_{\dot{\alpha}} & 0 \end{pmatrix}\,, \tag{2.19}$$

so that the six-dimensional spinors reduce to four-dimensional spinors.

We may also relate the six-dimensional polarization vectors (2.10) to four-dimensional ones. With four-dimensional reference spinors embedded as the above momenta, the states with $(a, \dot{a})$ either $(1, \dot{1})$ or $(2, \dot{2})$ correspond to positive and negative helicity states respectively. The mixed labels $(1, \dot{2})$ and $(2, \dot{1})$ appear as scalars from the four-dimensional point of view. Of course, the particular map between six-dimensional quantum numbers and helicities depends on the explicit embedding of four-dimensional spinors in the six-dimensional space.

C. Tree-amplitude examples

As usual, in this paper we will work with color-ordered amplitudes [33]. Applying the above helicity formulæ to the color-ordered four-gluon amplitude, one obtains a remarkably compact result [34],

$$A_4^{\rm tree}(1^g_{a\dot{a}}, 2^g_{b\dot{b}}, 3^g_{c\dot{c}}, 4^g_{d\dot{d}}) = -\frac{i}{s_{12}s_{23}} \langle 1_a 2_b 3_c 4_d\rangle [1_{\dot{a}} 2_{\dot{b}} 3_{\dot{c}} 4_{\dot{d}}]\,, \tag{2.20}$$

where the inner products are defined in eq. (2.6). As another example, the two-chiral-quark two-gluon amplitude is just as simple and given by,

$$A_4^{\rm tree}(1^g_{a\dot a}, 2^g_{b\dot b}, 3^q_c, 4^q_d) = -\frac{i}{s_{12}s_{23}}\langle 1_a 2_b 3_c 4_d\rangle [1_{\dot a} 2_{\dot b} 3_{\dot e} 3^{\dot e}]\,, \tag{2.21}$$

where the repeated index "$\dot e$" on the right side is summed. Besides their remarkable simplicity, these formulæ exhibit a number of rather nice properties. In six dimensions, because the little group SU(2)×SU(2) connects all helicities together, there is no concept like maximally helicity violating (MHV) amplitudes: in terms of six-dimensional spinors a single formula describes the amplitude. This property is manifest in eq. (2.20).

The three-point amplitude is a bit trickier. Naively, the amplitude should contain an inverse of $\langle i_a|j_{\dot b}]$ which would be ill-defined because $\det\langle i_a|j_{\dot b}]$ vanishes for three-point kinematics. The solution worked out by Cheung and O'Connell is to introduce two-component objects $u_{ia}, \tilde u_{j\dot b}$ and $w_{ia}, \tilde w_{j\dot b}$. In terms of these, the three-point amplitude is given by,

$$A_3^{\rm tree}(1_{a\dot a}, 2_{b\dot b}, 3_{c\dot c}) = i\Gamma_{abc}\,\tilde\Gamma_{\dot a\dot b\dot c}\,, \tag{2.22}$$

where,

$$\begin{aligned}\Gamma_{abc} &= u_{1a}u_{2b}w_{3c} + u_{1a}w_{2b}u_{3c} + w_{1a}u_{2b}u_{3c}\,,\\ \tilde\Gamma_{\dot a\dot b\dot c} &= \tilde u_{1\dot a}\tilde u_{2\dot b}\tilde w_{3\dot c} + \tilde u_{1\dot a}\tilde w_{2\dot b}\tilde u_{3\dot c} + \tilde w_{1\dot a}\tilde u_{2\dot b}\tilde u_{3\dot c}\,.\end{aligned} \tag{2.23}$$

The definitions of the u and w objects may be found in ref. [34] and are summarized here in appendix B.

A striking property that can be observed in the three- and four-point amplitudes (2.20) and (2.22) is that they contain pairs of chiral-conjugate factors. In particular, for the four-gluon case, both chiral $\langle 1_a 2_b 3_c 4_d\rangle$ and antichiral $[1_{\dot a} 2_{\dot b} 3_{\dot c} 4_{\dot d}]$ factors appear in the numerator. Similarly, the fermionic amplitude (2.21) breaks up into a chiral and an antichiral factor.

D. Unitarity method and six-dimensional helicity

The modern unitarity method constructs loop amplitudes directly from on-shell tree amplitudes [1], by combining unitarity cuts into complete expressions for amplitudes. The most convenient cuts generally are those that reduce the loop amplitude integrands into a sum of products of tree amplitudes,

$$A_n^{\rm loop}\big|_{\rm cut} = \sum_{\rm states} A^{\rm tree}A^{\rm tree}\cdots A^{\rm tree}A^{\rm tree}\,. \tag{2.24}$$

To construct the full amplitude, we can apply a merging procedure for combining cuts [42]. For more complicated cases, it is best to build an ansatz first in terms of some arbitrary parameters. The arbitrary parameters are then determined by comparing the cuts of the ansatz against the generalized unitarity cuts (2.24). If an inconsistency is found, the ansatz is not general enough and must be enlarged. In four dimensions, a particularly simple set of cuts to evaluate is those with the maximal numbers of cut propagators [23]. Often it is convenient to build the ansatz for the amplitude by starting with generalizations of these types of maximal cuts and then systematically relaxing the cut conditions one at a time [12, 17, 47]. This approach, known as the method of maximal cuts, offers a systematic procedure for obtaining complete amplitudes, including nonplanar contributions, at any loop order in massless theories. One can carry out cut calculations either analytically or numerically comparing to a target ansatz at high precision.[3]

An important concept is "spanning cuts", or a complete set of cuts for determining an amplitude. For the color-ordered one-loop four-point amplitude a spanning set is the usual s and t channel two-particle cuts. More generally, spanning cuts are determined by requiring that all potential terms that can contribute, including contact terms, can be detected by the cuts. In section VI we use such a spanning set of cuts to confirm the six-dimensional validity of the complete four-loop four-point amplitude of $\mathcal{N}=4$ sYM theory, calculated in refs. [18, 47] using mostly four-dimensional methods.

---

[3] Since this procedure does not involve any integration, high precision is straightforward. One can also choose rational numbers for the kinematic points.

One of the key ingredients in evaluating unitarity cuts is to have kinematics that satisfies all cut conditions. At one loop, for explanatory purposes it is much more convenient to use analytic solutions of the cut conditions, as we do in section IV, while at higher loops, numerical solutions are generally easier to use. One-loop analytic solutions for the on-shell conditions for massless and massive cases have been discussed previously in refs. [23, 25–28, 31].

E. Comments on connection to massive regulators

For $\mathcal{N} = 4$ sYM theory in four dimensions, one can use a massive regulator, because the theory is only infrared divergent and not ultraviolet divergent. For planar amplitudes, a convenient massive Higgs regulator was recently proposed in ref. [48] for use in this theory. This regulator has the advantage of preserving the dual conformal invariance and also of leading to integrals that are much simpler to evaluate than their dimensionally regularized counterparts.

In general, we can instead view a massively regulated amplitude as a higher-dimensional one, but where we do not carry out the loop momentum integrations over the extra-dimensional components. This meshes well with our six-dimensional helicity implementation of the unitarity method. The gauge invariance of this construction is guaranteed by the gauge invariance of the constituent tree amplitudes appearing in the unitarity cuts.[4] To implement a massive regulator, we simply interpret the extra components in terms of masses, $\sum_{\mu=4}^{5} l_i^\mu l_{i\mu} \equiv -m_i^2$, taking on definite values that are not integrated. The key constraints on the allowed choices are that the underlying extra-dimensional components must satisfy the usual momentum conservation constraints and that all particles remain massless from the six-dimensional viewpoint. From the four-dimensional viewpoint, the on-shell condition is then, $\sum_{\mu=0}^{3} l_i^\mu l_{i\mu} \equiv m_i^2$. As emphasized in ref. [48], one particularly effective choice for planar amplitudes is to take a uniform mass in the outermost loop, while keeping all other legs massless.

In many cases, conversion of massless dimensionally regularized results to massive ones is straightforward [48]. However, in general, one would like to derive or confirm massively regulated integrands directly from unitarity cuts. In particular, our confirmation in section VI C that the functional form of the four-point four-loop amplitude is unchanged between four and six dimensions ensures that the straightforward conversion of this amplitude to a massively regulated form is compatible with unitarity. For six- and higher-point amplitudes, we know that the situation is a bit more complicated, because the higher-dimensional integrands contain additional pieces not detectable in four-dimensional massless cuts. Although such terms are expected to vanish as $m \to 0$ even after integration, they would be needed for studies of the Coulomb phase of the theory where the mass is kept finite.

III. A SIX-DIMENSIONAL STRUCTURE

As seen in section II C, three- and four-point tree amplitudes contain a pair of chiral-conjugate factors. How general is this? To answer this we turn to BCFW recursion relations [2], which offer a means for constructing tree amplitudes in a form where we can exploit the six-dimensional helicity techniques. It also provides a convenient means for generating tree amplitudes needed in the unitarity cuts.

A. BCFW recursion

The BCFW shift using six-dimensional spinor helicity was given in ref. [34], and the supersymmetric version in [43]. Here we give a brief summary and the relevant bosonic shifts. We begin by picking two external lines, say $1, 2$ as special, and deform them by a null vector proportional to a complex parameter z,

$$p_1(z) = p_1 + zr, \qquad p_2(z) = p_2 - zr\,, \tag{3.1}$$

where r is a null vector satisfying $p_1 \cdot r = p_2 \cdot r = 0$. These conditions ensure that the deformed momenta remain on-shell, $p_1^2(z) = p_2^2(z) = 0$, and the overall momentum conservation of the amplitude is unaltered.

[4] In theories with fewer supersymmetries, gauge invariance at the level of the integrand is complicated by the potential presence of terms such as bubbles on external legs, which are not detectable in the unitarity cuts.

Since a tree amplitude is a rational function of momenta with no more than a single pole in any given kinematic invariant, this deformation will result in a complex function with only simple poles in z. Each pole in z will correspond to a propagator that is a sum of a subset of external momenta that includes only one of the shifted momenta,

$$P_{2j}(z)^2 \equiv (p_2(z) + \ldots + p_j)^2 = P_{2j}^2 + 2zr \cdot P_{2j} \,. \tag{3.2}$$

The location of the pole is given by solving the on-shell condition $P_{2j}(z)^2 = 0$,

$$z_{2j} = -\frac{P_{2j}^2}{2r \cdot P_{2j}} \,. \tag{3.3}$$

As in common usage, we denote the shifted momenta evaluated at the value of z locating a pole with a hatted symbol " $\hat{}$ ", e.g. $\hat{p}_2 \equiv p_2(z = z_{2j})$.

If a shifted amplitude vanishes as $z \to \infty$, then standard complex variable theory implies that it is uniquely determined by its residues in z. For $D \geq 4$ dimensions, it is straightforward to find choices of shifts where this property holds for Yang-Mills theories [34, 51]. The poles correspond to configurations where propagators go on shell and where the amplitude factorizes into a product of lower-point amplitudes. Each residue is then simply a sum of products of two lower-point tree amplitudes on either side of the propagator, with the shifted momenta evaluated at the location of the pole. If legs 1 and 2 are shifted, the BCFW recursion relation gives us the unshifted amplitude as,

$$A_n^{\text{tree}}(0) = \sum_{j=3}^{n-1} \sum_h A_L\Big(\hat{p}_2, \ldots, p_j, -\hat{P}_{2j}^{(-h)}\Big) \frac{i}{P_{2j}^2} A_R\Big(\hat{P}_{2j}^{(h)}, p_{j+1}, \ldots, \hat{p}_1\Big)\Big|_{z=z_{2j}} \,, \tag{3.4}$$

where A_L and A_R are lower-point tree amplitudes on the left and right sides of the propagator and are evaluated at shifted momenta with $z = z_{2j}$. The first sum in the above equation is over all diagrams that produce poles, while the second is over all helicity states that cross the internal leg $\hat{P}$.

In six dimensions, the conditions $p_1 \cdot r = p_2 \cdot r = 0$ can be solved by choosing r to be proportional to the polarization of line 1, $r \sim \epsilon_{1a\dot{a}}$, and choosing the reference spinor for the polarization vector to be λ_2. This satisfies the needed constraints and leads to sufficiently good behavior at large z. Since $\epsilon_{1a\dot{a}}$ has extra SU(2)×SU(2) little-group indices, one introduces an auxiliary matrix $X^{a\dot{a}}$ to contract the indices so that,

$$r^{AB} = \frac{1}{\sqrt{2}} X^{a\dot{a}} (\epsilon_1^{AB})_{a\dot{a}} = -X^{a\dot{a}} \frac{\lambda_{1a}^{[A} \lambda_{2b}^{B]}}{[1^{\dot{a}}|2_b\rangle} = X^{a\dot{a}} \frac{{}^{[A}\not{p}_2 |1_{\dot{a}}] \langle 1_a|^{B]}}{s_{12}} \,, \tag{3.5}$$

and the condition $r^2 = 0$ now becomes $\det X = 0$. This can automatically be satisfied by choosing $X_{a\dot{a}} = x_a \tilde{x}_{\dot{a}}$, where the x_a and $\tilde{x}_{\dot{a}}$ are arbitrary. These arbitrary variables will cancel out once one sums over all contributions. When implementing the recursion relations numerically, these variables are helpful since they can identify errors when one checks whether the result is independent of the choice of x_a, $\tilde{x}_{\dot{a}}$. The above shift can be translated into a redefinition of the spinors,

$$\begin{aligned}
\lambda_1^{Aa}(z) &= \lambda_1^{Aa} - \frac{z}{s_{12}} X^a{}_{\dot{a}} [1^{\dot{a}}|2^b\rangle \lambda_{2b}^A \,, \qquad & \lambda_2^{Ab}(z) &= \lambda_2^{Ab} - \frac{z}{s_{12}} X^a{}_{\dot{a}} \lambda_{1a}^A [1^{\dot{a}}|2^b\rangle \,, \\
\tilde{\lambda}_{1A\dot{a}}(z) &= \tilde{\lambda}_{1A\dot{a}} + \frac{z}{s_{12}} X^a{}_{\dot{a}} \langle 1_a|2_{\dot{b}}] \tilde{\lambda}_{2A}^{\dot{b}} \,, \qquad & \tilde{\lambda}_{2A\dot{b}}(z) &= \tilde{\lambda}_{2A\dot{b}} + \frac{z}{s_{12}} X^a{}_{\dot{a}} \tilde{\lambda}_{1A}^{\dot{a}} \langle 1_a|2_{\dot{b}}] \,.
\end{aligned} \tag{3.6}$$

In section V B, we will describe the supersymmetrized BCFW recursion relations to generate the tree amplitudes needed in calculations of multiloop amplitudes of $\mathcal{N} = 4$ sYM theory.

B. A double copy

As noted in section II C, the three- and four-point amplitudes contain chiral-conjugate factors. An obvious question is whether this property can be extended to n points. Indeed this is the case, as can be seen using BCFW recursion relations. This can be understood by noting that six-dimensional on-shell helicity states of Yang-Mills theory transform under a representation of the little group which factorizes into the direct product of two spinor representations. That is, the helicity sum in eq. (3.4), can be rewritten as a product of two independent sums: $\sum_h \to \sum_a \times \sum_{\dot{a}}$. Thus, if the lower-point amplitudes in the numerator of eq. (3.4) can also be written as products, one factor carrying the undotted

SU(2) indices and the other carrying the dotted SU(2) indices, then the BCFW recursion relations will preserve this property for the higher-point amplitudes. Since the three and four-point amplitudes do have this property, it holds for any number of legs by recursively constructing the amplitudes.

For example, at five points, applying a BCFW recursion based on shifting legs 1 and 2, following the discussion of ref. [34], we obtain two contributions, one in the s_{23} channel and the other in the s_{51} channel. Evaluating the diagrams gives,

$$\begin{aligned} A_5^{\text{tree}}&(1_{a\dot{a}}, 2_{b\dot{b}}, 3_{c\dot{c}}, 4_{d\dot{d}}, 5_{e\dot{e}}) \\ &= -\frac{i}{s_{45}s_{5\hat{1}}s_{23}} \left(\langle \hat{1}_a \hat{2}_b 4_d 5_e\rangle u_{3c} + \langle \hat{1}_a 3_c 4_d 5_e\rangle u_{\hat{2}b}\right) \left(\left[\hat{1}_{\dot{a}} \hat{2}_{\dot{b}} 4_{\dot{d}} 5_{\dot{e}}\right] \tilde{u}_{3\dot{c}} + \left[\hat{1}_{\dot{a}} 3_{\dot{c}} 4_{\dot{d}} 5_{\dot{e}}\right] \tilde{u}_{\hat{2}\dot{b}}\right) \\ &\quad - \frac{i}{s_{34}s_{51}s_{\hat{2}3}} \left(\langle \hat{2}_b \hat{1}_a 4_d 3_c\rangle u_{5e} + \langle \hat{2}_b 5_e 4_d 3_c\rangle u_{\hat{1}a}\right) \left(\left[\hat{2}_{\dot{b}} \hat{1}_{\dot{a}} 4_{\dot{d}} 3_{\dot{c}}\right] \tilde{u}_{5\dot{e}} + \left[\hat{2}_{\dot{b}} 5_{\dot{e}} 4_{\dot{d}} 3_{\dot{c}}\right] \tilde{u}_{\hat{1}\dot{a}}\right) . \end{aligned} \tag{3.7}$$

We thus explicitly see that the chiral-conjugate nature of the three- and four-point amplitudes is inherited directly by the five-point amplitude via the BCFW recursion relations. As noted above, the hats indicate that the momenta are shifted as in eq. (3.1), with z evaluated at the value (3.3) for the two given channels. If we try to clean up the expression, for example by factoring out the auxiliary variables x^a, $\tilde{x}^{\dot{a}}$, we can easily hide the chiral-conjugate structure. By continuing the recursion and maintaining the BCFW format at each level of the recursion, we straightforwardly obtain forms where chiral-conjugate factors appear in each term at n points.

This behavior has some similarities with the double-copy structure for gravity amplitudes uncovered by two of the authors and Johansson (BCJ) in ref. [4]. In that case, numerators of gravity diagrams appear as two factors of gauge theory numerators. There are, however, also important differences between the two cases. The most obvious one is that in the gravity case no chiral conjugation is needed for one of the copies. More importantly, for the case of gravity, we can interpret the factors as pieces of physical Yang-Mills amplitudes, but for the present case of Yang-Mills theory we do not have an interpretation in terms of amplitudes of some theory. In fact, it is unclear how to write down a Lagrangian that would lead to only one of the factors of the three-point Yang-Mills amplitude, either Γ_{abc} or $\tilde{\Gamma}_{\dot{a}\dot{b}\dot{c}}$. This may be contrasted with the gravity case where there is a partial Lagrangian understanding [52]. Another difference is that the gravity double copy relies on a group-theory Jacobi identity structure in the gauge-theory diagram kinematic numerators [4]. Such a structure is not apparent in the present case. Nevertheless, the present structure can be helpful in computations.

IV. EXAMPLE: ONE-LOOP QCD AMPLITUDES

Our task in this section is to demonstrate how six-dimensional helicity methods can be combined with the unitarity method to obtain complete one-loop QCD amplitudes. We take external momenta and helicities to live in a four-dimensional subspace, but take the internal momenta to be six dimensional. In general, any dimensionally regularized massless amplitude can be expressed as a linear combination of scalar box, triangle, and bubble integrals with rational coefficients [53]. Since these integrals are known, the problem is reduced to determining the rational coefficients of the integrals. Here we choose a slightly different representation allowing also integrals with arbitrary powers of $m\tilde{m}$ in their numerators, following refs. [21, 31].

A. One-loop four-point cut conditions in $D = 6$

For the purposes of obtaining one-loop QCD amplitudes, we take the external legs to carry massless four-dimensional momenta and the loop to carry six-dimensional momentum. To solve the cut conditions, we view the massless six-dimensional loop momentum as massive four-dimensional momentum. The mass parameter is then conserved, as inherited from the six-dimensional momentum components. To solve for the cut conditions, we consider a particle with a uniform mass around the loop.

To illustrate six-dimensional helicity, we consider the simple case of four massless external legs. We start with the quadruple cut displayed in fig. 1(a). In this case, we must solve the cut conditions ${}^{(4)}l_i^2 = m\tilde{m}$, where ${}^{(4)}l$ denotes a momentum vector keeping only the first four components. In this case we can find a solution for the first four components of the loop momentum vectors, in terms of purely four-dimensional spinors,

$$({}^{(4)}l^{\pm})_1^{\mu} \;=\; \frac{1}{2}\left(c_1^{\pm} \left\langle 4^- \right| \gamma^{\mu} \left| 1^- \right\rangle - \frac{1}{c_1^{\pm}} \frac{m\tilde{m}}{s_{14}} \left\langle 1^- \right| \gamma^{\mu} \left| 4^- \right\rangle\right) , \qquad \mu = 0, 1, 2, 3 \tag{4.1}$$

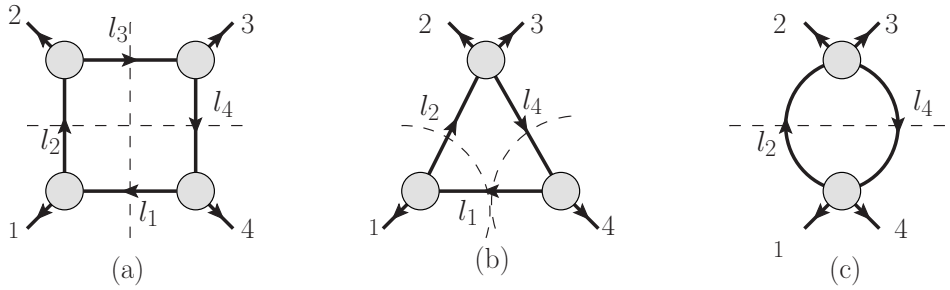

FIG. 1: Cuts used to obtain a one-loop four-point amplitude. We display the triple cuts and ordinary two-particle cut in the s_{14} channel. In general, we must also evaluate s_{12} channel cuts.

where,

$$c_1^{\pm} = \frac{\langle 1\,2\rangle}{2\,\langle 4\,2\rangle}\left(1 \pm \sqrt{1 + \frac{4m\tilde{m}s_{24}}{s_{23}s_{34}}}\right) . \tag{4.2}$$

Although there are two solutions to the quadruple cuts, in general, when summing over these the square root drops out.

The fifth and sixth dimensional components of the loop momenta are

$$l_i^4 = \frac{-m+\tilde{m}}{2i}\,, \qquad\qquad l_i^5 = \frac{m+\tilde{m}}{2}\,. \tag{4.3}$$

The other momenta in the loop are given by momentum conservation $l_2 = l_1 - p_1$, $l_3 = l_1 - p_1 - p_2$ and $l_4 = l_1 + p_4$. Because of the symmetry in the problem we can also obtain these momenta from relabellings of eq. (4.1). If viewed as massive momenta in four dimensions, m and $\tilde{m}$ are constants, and the momenta (4.1) are two independent solutions to the cut conditions. In contrast, when interpreted as six-dimensional momenta, (4.1) together with (4.3) are not constrained completely by the cut conditions. Their remaining freedom is parametrized by the now dynamic mass parameters m and $\tilde{m}$. In fact, what we labeled as two parameters can be thought of as a single complex parameter family of solutions.

Now consider the triple cut displayed in fig. 1(b). We note that,

$${}^{(4)}l_1^{\mu} = \frac{1}{2}\left(t\,\langle 4^-|\,\gamma^{\mu}\,|1^-\rangle - \frac{1}{t}\,\frac{m\tilde{m}}{s_{14}}\,\langle 1^-|\,\gamma^{\mu}\,|4^-\rangle\right) , \tag{4.4}$$

solves the three cut conditions ${}^{(4)}l_1^2 = {}^{(4)}l_2^2 = {}^{(4)}l_4^2 = m\tilde{m}$, where t is a parameter describing the remaining degree of freedom (from the four-dimensional vantage point) not frozen by the cut conditions. The other two cut momenta are specified by momentum conservation, $l_2 = l_1 - p_1$ and $l_4 = l_1 + p_4$. Again it is simple to check that the cut legs all satisfy the proper six-dimensional on-shell conditions.

We note that the similarity of the triple cut solution to the quadruple cut solutions is not accidental. Indeed if we demand that a fourth propagator goes on shell, ${}^{(4)}l_3^2 - m\tilde{m} = l_3^2 = (l_1 - p_1 - p_2)^2 \to 0$, this has the effect converting the triple cut into a quadruple cut. That is, we demand,

$$0 = (l_1 - p_1 - p_2)^2 = t\,\langle 4\,2\rangle\,[1\,2] + s_{12} - \frac{m\tilde{m}}{ts_{14}}\,\langle 1\,2\rangle\,[4\,2]\,. \tag{4.5}$$

Solving for t gives,

$$t_0 = \frac{\langle 1\,2\rangle}{2\,\langle 4\,2\rangle}\left(1 \pm \sqrt{1 + \frac{4m\tilde{m}s_{24}}{s_{14}s_{12}}}\right) , \tag{4.6}$$

matching $c_1^{\pm}$ in eq. (4.2).

B. One-loop four-point solution of six-dimensional spinors

Given the solution of the cut conditions above, it is then a simple matter to insert these into our solution for the six-dimensional spinors in terms of four-dimensional ones. To illustrate this, consider the triple cut displayed in fig. 1(b). To make the process simpler, it is convenient to express the four-dimensional momentum solutions in two-component notation. Taking the solution (4.4) and rewriting it in two-component notation, we have,

$$\begin{aligned}
{}^{(4)}l_1 &= t\lambda_4\tilde{\lambda}_1 - \frac{1}{t}\frac{m\tilde{m}}{s_{14}}\lambda_1\tilde{\lambda}_4\,,\\
{}^{(4)}l_2 &= \left(\lambda_4 - \frac{1}{t}\,\lambda_1\right)t\tilde{\lambda}_1 - \frac{m\tilde{m}}{ts_{14}}\lambda_1\,\tilde{\lambda}_4\,,\\
{}^{(4)}l_4 &= \lambda_4\left(\tilde{\lambda}_4 + t\,\tilde{\lambda}_1\right) - \frac{m\tilde{m}}{ts_{14}}\lambda_1\,\tilde{\lambda}_4\,.
\end{aligned} \tag{4.7}$$

To arrange the six-dimensional spinors for the loop momentum in terms of four-dimensional ones, we make use of the decomposition in eqs. (2.15) and (2.16). Comparing l_1 in eq. (4.7) to eq. (2.15), we see that in this case,

$$\begin{aligned}
&\mu = \lambda_1\,, \quad \tilde{\mu} = \frac{\tilde{\lambda}_4}{t}\,, \quad \lambda = \lambda_4\,, \quad \tilde{\lambda} = t\tilde{\lambda}_1\,,\\
&\kappa_{14} = \frac{m}{\langle 1\,4\rangle}\,, \quad \tilde{\kappa}_{14} = \frac{\tilde{m}}{[1\,4]}\,, \quad \kappa'_{14} = \frac{\tilde{m}}{\langle 1\,4\rangle}\,, \quad \tilde{\kappa}'_{14} = \frac{m}{[1\,4]}\,.
\end{aligned} \tag{4.8}$$

Plugging this into eq. (2.17) immediately gives us the six-dimensional spinors corresponding to l_1 as,

$$(\lambda_{l_1})^A{}_a = \begin{pmatrix} -\kappa_{14}\lambda_1 & \lambda_4 \\ t\tilde{\lambda}_1 & \tilde{\kappa}_{14}\tilde{\lambda}_4/t \end{pmatrix}, \qquad (\tilde{\lambda}_{l_1})_{A\dot{a}} = \begin{pmatrix} \kappa'_{14}\lambda_1 & \lambda_4 \\ -t\tilde{\lambda}_1 & \tilde{\kappa}'_{14}\tilde{\lambda}_4/t \end{pmatrix}. \tag{4.9}$$

Similarly, for the spinors carrying momenta l_2 and l_4 — needed for evaluating the triple cut in fig. 1(b) — we have

$$\begin{aligned}
(\lambda_{l_4})^A{}_a &= \begin{pmatrix} -\kappa_{14}\lambda_1 & \lambda_4 \\ \tilde{\lambda}_4 + t\tilde{\lambda}_1 & \tilde{\kappa}_{14}\tilde{\lambda}_4/t \end{pmatrix}, & (\tilde{\lambda}_{l_4})_{A\dot{a}} &= \begin{pmatrix} \kappa'_{14}\lambda_1 & \lambda_4 \\ -\tilde{\lambda}_4 - t\tilde{\lambda}_1 & \tilde{\kappa}'_{14}\tilde{\lambda}_4/t \end{pmatrix},\\
(\lambda_{l_2})^A{}_a &= \begin{pmatrix} -\kappa_{14}\lambda_1 & \lambda_4 - \lambda_1/t \\ t\tilde{\lambda}_1 & \tilde{\kappa}_{14}\tilde{\lambda}_4/t \end{pmatrix}, & (\tilde{\lambda}_{l_2})_{A\dot{a}} &= \begin{pmatrix} \kappa'_{14}\lambda_1 & \lambda_4 - \lambda_1/t \\ -t\tilde{\lambda}_1 & \tilde{\kappa}'_{14}\tilde{\lambda}_4/t \end{pmatrix}.
\end{aligned} \tag{4.10}$$

In many cases, we find ourselves with an incoming momentum, and as such it is labelled $-p$ in our all-outgoing convention. A simple prescription which preserves the relation between spinors and momenta and which is sufficient for purely gluonic amplitudes is to simply take $\lambda_{-p} = i\lambda_p$ and $\tilde{\lambda}_{-p} = i\tilde{\lambda}_p$. A similar prescription for any state in the $\mathcal{N} = 4$ supermultiplet will be given in section V.

Using this it is then a simple matter to work out the result for the cut. For the s_{14}-channel cut we have, if legs 1 and 4 are of positive helicity,

$$\begin{aligned}
\langle(-l_4)_1, 4_1, 1_1, (l_2)_1\rangle &= \det\begin{pmatrix} -i\kappa_{14}\lambda_1 & 0 & 0 & -\kappa_{14}\lambda_1 \\ i\tilde{\lambda}_4 + it\tilde{\lambda}_1 & \tilde{\lambda}_4 & \tilde{\lambda}_1 & t\tilde{\lambda}_1 \end{pmatrix} = 0\,,\\
\langle(-l_4)_1, 4_1, 1_1, (l_2)_2\rangle &= \det\begin{pmatrix} -i\kappa_{14}\lambda_1 & 0 & 0 & \lambda_4 - \lambda_1/t \\ i\tilde{\lambda}_4 + it\tilde{\lambda}_1 & \tilde{\lambda}_4 & \tilde{\lambda}_1 & \tilde{\kappa}_{14}\tilde{\lambda}_4/t \end{pmatrix} = i\kappa_{14}\,\langle 1\,4\rangle\,[4\,1]\,,\\
\langle(-l_4)_2, 4_1, 1_1, (l_2)_1\rangle &= \det\begin{pmatrix} i\lambda_4 & 0 & 0 & -\kappa_{14}\lambda_1 \\ i\tilde{\kappa}_{14}\tilde{\lambda}_4/t & \tilde{\lambda}_4 & \tilde{\lambda}_1 & t\tilde{\lambda}_1 \end{pmatrix} = -i\kappa_{14}\,\langle 1\,4\rangle\,[4\,1]\,,\\
\langle(-l_4)_2, 4_1, 1_1, (l_2)_2\rangle &= \det\begin{pmatrix} i\lambda_4 & 0 & 0 & \lambda_4 - \lambda_1/t \\ i\tilde{\kappa}_{14}\tilde{\lambda}_4/t & \tilde{\lambda}_4 & \tilde{\lambda}_1 & \tilde{\kappa}_{14}\tilde{\lambda}_4/t \end{pmatrix} = -i\frac{\langle 1\,4\rangle\,[4\,1]}{t}\,.
\end{aligned} \tag{4.11}$$

As seen from eqs. (2.6) and (2.17), the self-conjugate structure implies that the bracket expression is basically the same as the angle expression, except for the replacement $\kappa_{14} \to \kappa'_{14}$ along with some signs,

$$\begin{aligned}
&[(-l_2)_{\dot{1}}, 4_{\dot{1}}, 1_{\dot{1}}, (l_4)_{\dot{1}}] = 0\,, && [(-l_2)_{\dot{1}}, 4_{\dot{1}}, 1_{\dot{1}}, (l_4)_{\dot{2}}] = -i\kappa'_{14}\,\langle 1\,4\rangle\,[4\,1]\,,\\
&[(-l_2)_{\dot{2}}, 4_{\dot{1}}, 1_{\dot{1}}, (l_4)_{\dot{1}}] = i\kappa'_{14}\,\langle 1\,4\rangle\,[4\,1]\,, && [(-l_2)_{\dot{2}}, 4_{\dot{1}}, 1_{\dot{1}}, (l_4)_{\dot{2}}] = -i\frac{\langle 1\,4\rangle\,[4\,1]}{t}\,.
\end{aligned} \tag{4.12}$$

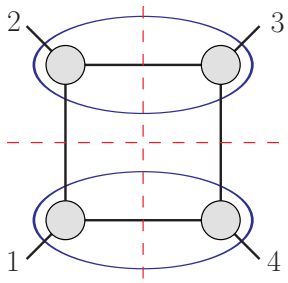

FIG. 2: The quadruple cut. The cuts are indicated by dashed (red) lines. Here two pairs of three-point amplitudes are grouped together to form two easier-to-use four-point tree amplitudes, indicated by the (blue) ovals. The cut propagators of the four-point tree amplitudes are canceled by multiplying by inverse propagators prior to imposing cut conditions.

Similarly, if leg 1 is of negative helicity and leg 2 of positive, we have,

$$\begin{aligned}
\langle(-l_4)_1, 4_1, 1_2, (l_2)_1\rangle &= \det\begin{pmatrix} -i\kappa_{14}\lambda_1 & 0 & \lambda_1 & -\kappa_{14}\lambda_1 \\ i\tilde{\lambda}_4 + it\tilde{\lambda}_1 & \tilde{\lambda}_4 & 0 & t\tilde{\lambda}_1 \end{pmatrix} = 0\,, \\
\langle(-l_4)_1, 4_1, 1_2, (l_2)_2\rangle &= \det\begin{pmatrix} -i\kappa_{14}\lambda_1 & 0 & \lambda_1 & \lambda_4 - \lambda_1/t \\ i\tilde{\lambda}_4 + it\tilde{\lambda}_1 & \tilde{\lambda}_4 & 0 & \tilde{\kappa}_{14}\tilde{\lambda}_4/t \end{pmatrix} = i\,\langle 1\,4\rangle\,[4\,1]\,t\,, \\
\langle(-l_4)_2, 4_1, 1_2, (l_2)_1\rangle &= \det\begin{pmatrix} i\lambda_4 & 0 & \lambda_1 & -\kappa_{14}\lambda_1 \\ i\tilde{\kappa}_{14}\tilde{\lambda}_4/t & \tilde{\lambda}_4 & 0 & t\tilde{\lambda}_1 \end{pmatrix} = -i\,\langle 1\,4\rangle\,[4\,1]\,t\,, \\
\langle(-l_4)_2, 4_1, 1_2, (l_2)_2\rangle &= \det\begin{pmatrix} i\lambda_4 & 0 & \lambda_1 & \lambda_4 - \lambda_1/t \\ i\tilde{\kappa}_{14}\tilde{\lambda}_4/t & \tilde{\lambda}_4 & 0 & \tilde{\kappa}_{14}\tilde{\lambda}_4/t \end{pmatrix} = 0\,,
\end{aligned} \tag{4.13}$$

and for the chiral conjugate,

$$\begin{aligned}
&[(-l_4)_{\dot{1}}, 4_{\dot{1}}, 1_{\dot{2}}, (l_2)_{\dot{1}}] = 0\,, && [(-l_4)_{\dot{1}}, 4_{\dot{1}}, 1_{\dot{2}}, (l_2)_{\dot{2}}] = i\,\langle 1\,4\rangle\,[4\,1]\,t\,, \\
&[(-l_4)_{\dot{2}}, 4_{\dot{1}}, 1_{\dot{2}}, (l_2)_{\dot{1}}] = -i\,\langle 1\,4\rangle\,[4\,1]\,t\,, && [(-l_4)_{\dot{2}}, 4_{\dot{1}}, 1_{\dot{2}}, (l_2)_{\dot{2}}] = 0\,.
\end{aligned} \tag{4.14}$$

This solution is valid as well for quadruple cuts by substituting $t \to t_0$ from eq. (4.6).

Similarly, the six-dimensional spinors can be solved for explicitly for any one-loop cuts with any number of external legs, although we refrain from giving the solutions here. These solutions are closely connected to the solutions of the cut conditions in four dimensions with masses [23, 28, 31].

C. QCD Calculations

By treating the extra-dimensional components of loop momenta effectively as masses to be integrated over, we can make use of four-dimensional methods for evaluating the coefficients of the integrals. The box coefficients are obtained by using the four on-shell conditions to freeze four components of loop momenta [23]. For the triangle and bubble integrals, we can use the approach of refs. [27, 31].

As a warmup we consider the simplest one-loop QCD amplitudes, with four identical-helicity external gluons in a four-dimensional subspace. This amplitude is especially simple because it can be determined entirely from the quadruple cut illustrated in fig. 2, where all four propagators are placed on shell. This follows from the property that in both two-particle cuts the four-point tree amplitudes on either side of the cut are each proportional to $m\tilde{m}$. Thus the numerator of the integrand must be proportional to $(m\tilde{m})^2$, saturating the dimensions of the numerator polynomial. Since this factor does not vanish when all four box propagators are placed on shell, the quadruple cut is sufficient for constructing the entire amplitude.

As discussed in section II C, four-point tree amplitudes expressed in terms of six-dimensional spinor helicity are simpler than their three-point counterparts. In general, this makes it advantageous to group three-point amplitudes appearing in the cuts into four-point amplitudes, but with the cut propagators removed by multiplying by the appropriate inverse propagators. With the grouping illustrated in fig. 2 by the (blue) ovals, we have the quadruple

cut as,

$$C_{1234} = \sum_{\text{states}} (-i)^2 (l_2 - p_2)^2 (l_2 + p_1)^2 \, A_4(-l_2, 2^+, 3^+, l_4) \, A_4(-l_4, 4^+, 1^+, l_2) \tag{4.15}$$
$$= \frac{\langle (-l_2)_a, 2_1, 3_1, (l_4)_b \rangle \, [(-l_2)_{\dot{a}}, 2_{\dot{1}}, 3_{\dot{1}}, (l_4)_{\dot{b}}] \, \langle (-l_4)^a, 4_1, 1_1, (l_2)^b \rangle \, [(-l_4)^{\dot{a}}, 4_{\dot{1}}, 1_{\dot{1}}, (l_2)^{\dot{b}}]}{s_{14} s_{23}} \,.$$

In general, we will label the generalized cuts with the indices i of l_i labeling the propagators; here all four propagators carrying momenta l_1, l_2, l_3 and l_4 are cut. We also assigned SU(2)×SU(2) little group indices $a, \dot{a} = 1$ to the external legs so that they carry positive helicity in the four-dimensional subspace.

Using the solution of the inner products given in eq. (4.11), relabeled for the other side of the cut, the quadruple cut in eq. (4.15) gives,

$$C_{1234} = 4 \frac{1}{s_{23} s_{14}} \kappa_{41} \kappa_{23} \kappa'_{41} \kappa'_{23} \langle 1\,4 \rangle^2 [4\,1]^2 \langle 3\,2 \rangle^2 [2\,3]^2$$
$$= 4 (m\tilde{m})^2 \frac{[2\,3]\,[1\,4]}{\langle 2\,3 \rangle \langle 1\,4 \rangle} = 4 (m\tilde{m})^2 \frac{[1\,2]\,[3\,4]}{\langle 1\,2 \rangle \langle 3\,4 \rangle} \,. \tag{4.16}$$

For this helicity configuration, the parameter t (which in the quadruple cut takes on the value t_0 in eq. (4.6)) drops out, leading to a rather simple result.

To obtain dimensionally regularized results we need to adjust the state sum. Such adjustments have been discussed in refs. [21, 54] and more recently in some detail in the context of QCD calculations making use of six dimensions [30]. Since we are working in six dimensions, there are $6 - 2 = 4$ gluon states circulating in the loop. This needs to be modified to match dimensional regularization. Two popular schemes are the 't Hooft-Veltman scheme [55], where $2(1 - \epsilon)$ gluon states circulate in the loop, and the four-dimensional helicity (FDH) scheme [54], where two states circulate. It is therefore convenient to take the number of states to be $2(1 - \delta_R \epsilon)$, where δ_R is unity for the 't Hooft-Veltman scheme and zero for the FDH scheme.

For our sample amplitude, since all four six-dimensional states give identical contributions, the adjustment amounts to simply changing the overall prefactor from $4 \to 2(1 - \delta_R \epsilon)$. We also need to adjust the number of components of extra-dimensional momenta from six to $D = 4 - 2\epsilon$. To do so we replace $m\tilde{m} \to \mu^2$, where μ is understood to carry (-2ϵ)-dimensional components of momentum. With these replacements, we obtain the dimensionally regularized result for the quadruple cut,

$$C_{1234} = 2(1 - \delta_R \epsilon) \mu^4 \frac{[1\,2]\,[3\,4]}{\langle 1\,2 \rangle \langle 3\,4 \rangle} \,. \tag{4.17}$$

Since the identical helicity amplitude is determined entirely from the quadruple cut, we obtain the dimensionally regularized amplitude by putting back the four cut propagators and integrating over the loop momentum in $4 - 2\epsilon$ dimensions. This gives,

$$A^{\text{1-loop}}(1^+, 2^+, 3^+, 4^+) = 2(1 - \epsilon \delta_R) \frac{[1\,2]\,[3\,4]}{\langle 1\,2 \rangle \langle 3\,4 \rangle} I_4[\mu^4] \,, \tag{4.18}$$

where the box integral is

$$I_4[\mathcal{P}] = \int \frac{d^{4-2\epsilon} l}{(2\pi)^{4-2\epsilon}} \frac{\mathcal{P}}{l^2 (l - p_1)^2 (l - p_1 - p_2)^2 (l + p_4)^2} \,, \tag{4.19}$$

with $\mathcal{P}$ a numerator polynomial. This result matches the known expression from ref. [21].

As a slightly more intricate example, consider the case where one external gluon carries negative helicity and the others positive helicity. As before, the quadruple cuts and triple cuts are conveniently extracted from the two-particle cuts, since these involve the simpler four-point tree amplitudes instead of three-point ones. Following similar logic as for the identical-helicity case (4.15), for the present case the quadruple cut, illustrated in fig. 1(a), is given by,

$$C_{1234} = \frac{1}{s_{14} s_{23}} \langle (-l_2)_a, 2_1, 3_1, (l_4)_b \rangle \, [(-l_2)_{\dot{a}}, 2_{\dot{1}}, 3_{\dot{1}}, (l_4)_{\dot{b}}]$$
$$\times \langle (-l_4)^a, 4_1, 1_2, (l_2)^b \rangle \, [(-l_4)^{\dot{a}}, 4_{\dot{1}}, 1_{\dot{2}}, (l_2)^{\dot{b}}] \,. \tag{4.20}$$

We then substitute in the solution for the spinor products, given in eqs. (4.11) and (4.13), appropriately relabeled and with the parameter t fixed to the quadruple cut value t_0 given in eq. (4.6). Summing over the internal helicity states then gives

$$\begin{aligned} C_{1234} &= -4\frac{\kappa_{23}\kappa'_{23}\,\langle 1\,4\rangle^2\,[4\,1]^2\,\langle 3\,2\rangle^2\,[2\,3]^2\;t_0^2}{s_{23}^2} \\ &= 4\frac{m\tilde{m}\,[2\,4]^2}{[1\,2]\,\langle 2\,3\rangle\,\langle 3\,4\rangle\,[4\,1]}\frac{s_{12}s_{23}}{s_{24}}\left(\frac{s_{23}s_{12}}{2s_{24}} + m\tilde{m} \pm \frac{s_{23}s_{12}}{2s_{24}}\sqrt{1+\frac{4m\tilde{m}s_{24}}{s_{23}s_{34}}}\right). \end{aligned} \tag{4.21}$$

As for the identical helicity case, each of the four states gives an identical result, so the dimensionally regularized result is obtained by replacing the overall prefactor of 4 by $2(1-\epsilon\delta_R)$ and substituting $m\tilde{m} \to \mu^2$. The box contribution is given by the sum over both solutions (normalized by a factor of $1/2$), so the square root drops out. Restoring the cut propagators and putting in the loop integration gives the box contribution to the amplitude,

$$A(1^-,2^+,3^+,4^+)\Big|_{\rm box} = 2(1-\delta_R\epsilon)\frac{[2\,4]^2}{[1\,2]\,\langle 2\,3\rangle\,\langle 3\,4\rangle\,[4\,1]}\frac{s_{12}s_{23}}{s_{13}}\left(\frac{s_{12}s_{23}}{2s_{13}}I_4[\mu^2] + I_4[\mu^4]\right), \tag{4.22}$$

where the box integrals are defined in eq. (4.19).

The triple cut of fig. 1(b) is also simple to obtain from the two-particle cut in fig. 1(c) by grouping the three-point trees together. After modifying the state sum this gives,

$$\begin{aligned} C_{124} &= -2(1-\epsilon\delta_R)\frac{\kappa_{23}\kappa'_{23}\,\langle 1\,4\rangle^2\,[4\,1]^2\,\langle 2\,3\rangle^2\,[3\,2]^2\;t^2}{s_{23}^2}\frac{i}{(l_1-p_1-p_2)^2} \\ &= -2i(1-\epsilon\delta_R)m\tilde{m}\,[2\,3]^2\,t^2\Big(t\;\langle 4\,2\rangle\,[1\,2] + s_{12} - \frac{m\tilde{m}}{ts_{14}}\,\langle 1\,2\rangle\,[4\,2]\Big)^{-1}. \end{aligned} \tag{4.23}$$

We used eq. (4.4) to express $l_1-p_1-p_2$ in terms of the parameter t. In this form the corresponding triangle coefficient can be extracted from the triple cut following refs. [27, 31]. Similarly, starting from the two-particle cuts, we can obtain the coefficients of bubble integrals. With this procedure, we can keep all terms which contribute to rational terms in the amplitudes.

In summary, this illustrates the use of six-dimensional helicity in unitarity cuts to obtain generalized cuts of one-loop amplitudes in QCD, which can then be reduced to a basis set of integrals using on-shell methods [26, 27, 30, 31]. Further details for converting state sums from six dimensions to their dimensionally regularized values may be found in ref. [30].

V. TREE-LEVEL MAXIMALLY SUPERSYMMETRIC YANG-MILLS AMPLITUDES

In this section we will describe tree-level amplitudes in $\mathcal{N}=4$ sYM theory using the recently constructed DHS on-shell superspace in six dimensions [43], as a precursor to carrying out multiloop calculations via the unitarity method in the next section. In particular, we will describe a convenient means for setting up high-point super-BCFW recursion for use in unitarity cuts.

A. Tree-level amplitudes

In the DHS superspace formalism, the on-shell superfield appears as a polynomial in a pair of anticommuting coordinates $\eta_a, \tilde{\eta}^{\dot{a}}$ which carry SU(2)×SU(2) little group indices,

$$\begin{aligned} \Phi(\eta,\tilde{\eta}) &= \phi + \chi^a\eta_a + \phi'(\eta)^2 + \tilde{\chi}_{\dot{a}}\tilde{\eta}^{\dot{a}} + g^a{}_{\dot{a}}\eta_a\tilde{\eta}^{\dot{a}} + \tilde{\psi}_{\dot{a}}(\eta)^2\tilde{\eta}^{\dot{a}} \\ &\quad + \phi''(\tilde{\eta})^2 + \psi^a\eta_a(\tilde{\eta})^2 + \phi'''(\eta)^2(\tilde{\eta})^2\,, \end{aligned} \tag{5.1}$$

where $(\eta)^2 \equiv \frac{1}{2}\epsilon^{ab}\eta_b\eta_a$ and $(\tilde{\eta})^2 \equiv \frac{1}{2}\epsilon_{\dot{a}\dot{b}}\tilde{\eta}^{\dot{b}}\tilde{\eta}^{\dot{a}}$. Using these fields, we can obtain superamplitudes in the usual way. The different component amplitudes can be read off from their η expansions. For example, the four-gluon amplitude

$\langle g^a{}_{\dot a}(1)\, g^b{}_{\dot b}(2)\, g^c{}_{\dot c}(3)\, g^d{}_{\dot d}(4)\rangle$ appears as the coefficient of $\eta_{1a}\tilde\eta_1^{\dot a}\eta_{2b}\tilde\eta_2^{\dot b}\eta_{3c}\tilde\eta_3^{\dot c}\eta_{4d}\tilde\eta_4^{\dot d}$ in the four-point superamplitude $\mathcal{A}_4$. These amplitudes are functions of momenta p_i and supermomenta $q_i, \tilde q_i$ defined by,

$$q_i^A = \lambda_i^{Aa}\eta_{ia}, \qquad \tilde q_{iB} = \tilde\lambda_{iB\dot b}\tilde\eta_i^{\dot b}\,. \tag{5.2}$$

For a general discussion of higher-dimensional on-shell superspaces, see ref. [44].

In ref. [43], the three-, four- and five-particle tree-level superamplitudes were worked out analytically. Consider first the four-point superamplitude, which is the simplest case. This is given by

$$\mathcal{A}_4^{\rm tree}(1,2,3,4) \;=\; -\frac{i}{s_{12}s_{23}}\,\delta^4\Big(\sum_{i=1}^4 q_i^A\Big)\delta^4\Big(\sum_{i=1}^4 \tilde q_{iB}\Big)\,, \tag{5.3}$$

where the fermionic delta function is defined as,

$$\delta^4\Big(\textstyle\sum_i q_i^A\Big) \equiv \frac{1}{4!}\,\epsilon_{BCDE}\,\Big(\sum\nolimits_i q_i^B\Big)\Big(\sum\nolimits_i q_i^C\Big)\Big(\sum\nolimits_i q_i^D\Big)\Big(\sum\nolimits_i q_i^E\Big)\,, \tag{5.4}$$

and likewise for the antichiral supermomentum $\tilde q_A$. This expression makes manifest the chiral–antichiral structure noted in section III B for the non-supersymmetric case.

The three-point superamplitude is a bit more complicated and is given by,

$$\mathcal{A}_3^{\rm tree}(1,2,3) \;=\; -i\big(\mathbf{u}_1\mathbf{u}_2+\mathbf{u}_2\mathbf{u}_3+\mathbf{u}_3\mathbf{u}_1\big)\Big(\sum_{i=1}^3\mathbf{w}_i\Big)\big(\tilde{\mathbf{u}}_1\tilde{\mathbf{u}}_2+\tilde{\mathbf{u}}_2\tilde{\mathbf{u}}_3+\tilde{\mathbf{u}}_3\tilde{\mathbf{u}}_1\big)\Big(\sum_{i=1}^3\tilde{\mathbf{w}}_i\Big)\,, \tag{5.5}$$

where $\mathbf{u}_i$ and $\mathbf{w}_i$ are defined in terms of the u_i^a and w_i^a of appendix B as,

$$\mathbf{u}_i = u_i^a\eta_{ia}, \quad \tilde{\mathbf{u}}_i = \tilde u_{i\dot a}\tilde\eta_i^{\dot a}, \quad \mathbf{w}_i = w_i^a\eta_{ia}, \quad \tilde{\mathbf{w}}_i = \tilde w_{i\dot a}\tilde\eta_i^{\dot a}\,. \tag{5.6}$$

The expression in eq. (5.5) is equivalent to the form given in ref. [43], except that here the chiral-conjugate property has been made manifest; it is a product of a chiral factor and an antichiral factor. As discussed in section III, this property survives the BCFW recursion, since the states in the six-dimensional sYM theory factorize into a direct product.

The five-point tree-level superamplitude is

$$\begin{aligned}\mathcal{A}_5^{\rm tree} \;=\;& i\,\frac{\delta^4\Big(\sum_i q_i^A\Big)\delta^4\Big(\sum_i \tilde q_{iB}\Big)}{s_{12}s_{23}s_{34}s_{45}s_{51}}\Big\{q_1^A(p_2p_3p_4p_5)_A{}^B\tilde q_{1B} + \text{cyclic}\\ &+\frac{1}{2}\Big[q_1^A\tilde\Delta_{2A}+q_3^A\tilde\Delta_{4A}+(q_3+q_4)^A\tilde\Delta_{5A}+(\text{chiral conjugate})\Big]\Big\}\,,\end{aligned} \tag{5.7}$$

where $\tilde\Delta_{2A} = (p_2p_3p_4p_5 - p_2p_5p_4p_3)_A{}^B\tilde q_{2B}$, $\tilde\Delta_{4A} = (p_4p_5p_1p_2 - p_4p_2p_1p_5)_A{}^B\tilde q_{4B}$, etc. The five-particle amplitude is given here in a particularly compact form which lacks explicit cyclic symmetry, although the symmetry does hold on the support of the fermionic delta functions.

An important distinction between the DHS on-shell superspace and the four-dimensional daughter theory is that this superspace is non-chiral. The interesting consequence of this feature is that while the four-dimensional amplitudes are organized according to N^{k}MHV categories, these all come from a single six-dimensional parent amplitude. This simplicity, however, is offset by the fact that one lacks the counterpart of the four-dimensional MHV amplitudes, which have a simple form for arbitrary numbers of legs.

B. Supersymmetric BCFW recursion

In order to investigate high loop orders we need high-point tree amplitudes. To obtain these, we use supersymmetric forms of the BCFW recursion relations. This also serves as a warmup for the unitarity cuts, because the state sums generated by integration over Grassmann parameters at loop level are similar to the state sums in supersymmetric forms of the BCFW recursion relations. As discussed in ref. [43], the super-BCFW recursion relations can be obtained by shifting the Grassmann variables,

$$\begin{aligned}\eta_{1a}(z) \;&=\; \eta_{1a} - zX_{a\dot a}[1^{\dot a}|2^b\rangle\eta_{2b}/s_{12}\,, & \eta_{2b}(z) &= \eta_{2b} - zX^a{}_{\dot a}[1^{\dot a}|2_b\rangle\eta_{1a}/s_{12}\,,\\ \tilde\eta_1^{\dot a}(z) \;&=\; \tilde\eta_1^{\dot a} + zX^{a\dot a}[2_{\dot b}|1_a\rangle\tilde\eta_2^{\dot b}/s_{12}\,, & \tilde\eta_2^{\dot b}(z) &= \tilde\eta_2^{\dot b} + zX^a{}_{\dot a}[2^{\dot b}|1_a\rangle\tilde\eta_1^{\dot a}/s_{12}\,,\end{aligned} \tag{5.8}$$

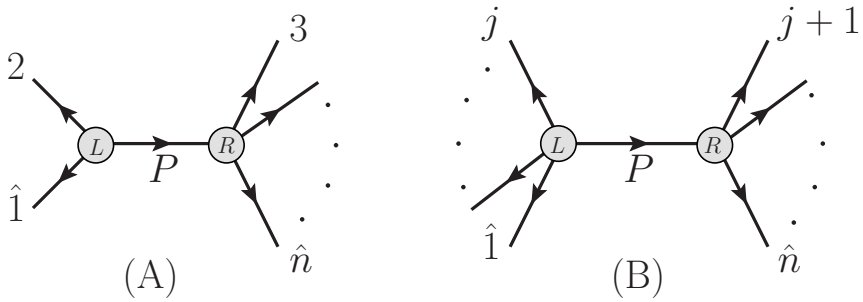

FIG. 3: Two categories of BCFW diagrams. (A) contains a three-point subamplitude, which does not have the full supermomentum delta function $\delta^4(q)\delta^4(\tilde{q})$. (B) contains no three-point subamplitude, thus all delta functions are of degree four.

in addition to the shifts of the spinors in eq. (3.6). This is designed to maintain supermomentum conservation, i.e. $q_1^A + q_2^A = q_{\hat{1}}^A + q_{\hat{2}}^A$ and $\tilde{q}_{1A} + \tilde{q}_{2A} = \tilde{q}_{\hat{1}A} + \tilde{q}_{\hat{2}A}$. These shifts on η can be rephrased as shifts directly on the supermomenta by combining with the spinorial shifts in eq. (3.6) and using the trick,

$$\delta^a{}_b = -\frac{1}{s_{12}}\langle 1^a|\not{p}_2|1_b\rangle\,. \tag{5.9}$$

After the rearrangements, we have,

$$\begin{aligned}
q_1^A(z) &= q_1^A + \frac{z}{s_{12}^2}X^a{}_{\dot{a}}[1^{\dot{a}}|2^b\rangle\lambda_{2b}^A\langle 1_a|2_{\dot{b}}]\tilde{\lambda}_{2B}^{\dot{b}}q_1^B - \frac{z}{s_{12}}\lambda_1^{Aa}X_{a\dot{a}}\tilde{\lambda}_{1B}^{\dot{a}}q_2^B\,,\\
q_2^A(z) &= q_2^A - \frac{z}{s_{12}}\lambda_{1a}^A X^a{}_{\dot{a}}\tilde{\lambda}_{1B}^{\dot{a}}q_2^B - \frac{z}{s_{12}^2}X^a{}_{\dot{a}}[1^{\dot{a}}|2_b\rangle\lambda_2^{Ab}\langle 1_a|2_{\dot{b}}]\tilde{\lambda}_{2B}^{\dot{b}}q_1^B\,,\\
\tilde{q}_{1A}(z) &= \tilde{q}_{1A} + \frac{z}{s_{12}^2}X^a{}_{\dot{a}}\langle 1_a|2_{\dot{b}}]\tilde{\lambda}_{2A}^{\dot{b}}[1^{\dot{a}}|2^b\rangle\lambda_{2b}^B\tilde{q}_{1B} + \frac{z}{s_{12}}\tilde{\lambda}_{1A\dot{a}}X^{a\dot{a}}\lambda_{1a}^B\tilde{q}_{2B}\,,\\
\tilde{q}_{2A}(z) &= \tilde{q}_{2A} + \frac{z}{s_{12}}X^a{}_{\dot{a}}\tilde{\lambda}_{1A}^{\dot{a}}\lambda_{1a}^B\tilde{q}_{2B} + \frac{z}{s_{12}^2}X^a{}_{\dot{a}}\tilde{\lambda}_{2A\dot{b}}[2^{\dot{b}}|1_a\rangle[1^{\dot{a}}|2^b\rangle\lambda_{2b}^B\tilde{q}_{1B}\,.
\end{aligned} \tag{5.10}$$

As we will see, these supermomentum shifts help us avoid dealing directly with the supercoordinates η in the recursion.

The intermediate state sum in the recursion is realized as an integration over the Grassmann coordinates $\eta_P, \tilde{\eta}_P$ of the intermediate leg (labeled as P), and the remainder of this section is devoted to systematically carrying out these integrations.

To set up high-point recursion, it is useful to first organize the types of contributions. If we track the factors containing Grassmann parameters, and drop other factors, the n-point tree amplitudes have the schematic form,

$$\mathcal{A}_n \;\sim\; \delta^4\Big(\sum\nolimits_i q_i^A\Big)\delta^4\Big(\sum\nolimits_i \tilde{q}_{iB}\Big)q^{n-4}\tilde{q}^{n-4} \quad \text{for } n \geq 4\,. \tag{5.11}$$

The supermomentum delta functions for $n \geq 4$ impose algebraic constraints on $\eta_P, \tilde{\eta}_P$ under the fermionic integration. We can follow the same strategy as used in four dimensions to consider the delta-function constraints as a set of algebraic equations to be systematically solved [38]. A key identity for carrying this out is

$$\delta^4(q_1^A + q_2^A + Q^A) \;=\; s_{12}\,\delta^2\Big(\eta_{1a} + s_{12}^{-1}\langle 1_a|\not{p}_2 Q\Big)\delta^2\Big(\eta_{2b} + s_{12}^{-1}\langle 2_b|\not{p}_1 Q\Big)\,. \tag{5.12}$$

A similar antichiral identity also holds. These identities are analogous to ones used in four dimensions [36].

Before proceeding, though, we are obliged to address a glitch in the spinor-helicity formalism: the spinors do not properly distinguish between particles and antiparticles, causing phase inconsistencies in diagrams containing fermions. This glitch and prescriptions for resolving it have already been discussed in the four-dimensional case, for example, in ref. [38, 56]. Here we use the prescription that if p is incoming, so that this momentum is $-p$ in our all-outgoing convention, then we take,

$$\lambda_{(-p)}^{Aa} \equiv i\lambda_p^{Aa}, \qquad \tilde{\lambda}_{(-p)A\dot{a}} \equiv i\tilde{\lambda}_{pA\dot{a}}\,. \tag{5.13}$$

In this way, we maintain the relationship between momenta and spinors, i.e.,

$$(-p)^{AB} = \lambda^{Aa}_{(-p)}\lambda^{B}_{(-p)a} = -\lambda^{Aa}_{p}\lambda^{B}_{pa}\,. \tag{5.14}$$

Along the same lines, we demand that $q^A_{(-p)} = -q^A_p$, which we achieve with the same prescription for the supercoordinates η: whenever $-p$ is outgoing, we choose,

$$\eta_{(-p)a} \equiv i\eta_{pa}, \qquad \tilde{\eta}^{\dot{a}}_{(-p)} \equiv i\tilde{\eta}^{\dot{a}}_{p}. \tag{5.15}$$

Beyond four points, we can split all BCFW diagrams into two categories, as shown in fig. 3. We consider these two cases in turn.

Case (A):

In cases where one has to sew a three-point superamplitude to a higher-point tree superamplitude, illustrated in fig. 3(A), the Grassmann integration has the form,

$$\int d^2\eta_P d^2\tilde{\eta}_P\ \mathcal{A}_{3L} \times \delta^4\Big(\sum_{i\in R} q_i^B\Big)\delta^4\Big(\sum_{i\in R}\tilde{q}_{iC}\Big)q^{n-5}\tilde{q}^{n-5}\,, \tag{5.16}$$

where the summations are over all external lines of the right tree amplitude including shifted legs, and the integration measure is $d^2\eta_P d^2\tilde{\eta}_P = \frac{1}{4}d\eta^a_P d\eta_{Pa} d\tilde{\eta}_{P\dot{a}} d\tilde{\eta}^{\dot{a}}_P$.

To perform this integral, we view the factors in the three-point amplitude (5.5) as algebraic constraints on the supercoordinates $\eta_P, \tilde{\eta}_P$ imposing,

$$\begin{aligned}
&\mathbf{u}_{\hat{1}} = \mathbf{u}_2\,, \qquad &&\mathbf{u}_P = \tfrac{1}{2}(\mathbf{u}_{\hat{1}} + \mathbf{u}_2), \qquad &&\mathbf{w}_P = -\mathbf{w}_{\hat{1}} - \mathbf{w}_2,\\
&\tilde{\mathbf{u}}_{\hat{1}} = \tilde{\mathbf{u}}_2\,, \qquad &&\tilde{\mathbf{u}}_P = \tfrac{1}{2}(\tilde{\mathbf{u}}_{\hat{1}} + \tilde{\mathbf{u}}_2), \qquad &&\tilde{\mathbf{w}}_P = -\tilde{\mathbf{w}}_{\hat{1}} - \tilde{\mathbf{w}}_2\,.
\end{aligned} \tag{5.17}$$

Since there are two components each in η_{Pa} and $\tilde{\eta}^{\dot{a}}_P$, the three-point amplitude is sufficient to localize the η_P integrals. The solutions to the constraint equations are

$$\begin{aligned}
\eta_{Pa} &= \tfrac{1}{2}w_{Pa}(\mathbf{u}_{\hat{1}} + \mathbf{u}_2) + u_{Pa}(\mathbf{w}_{\hat{1}} + \mathbf{w}_2)\,,\\
\tilde{\eta}^{\dot{a}}_P &= -\tfrac{1}{2}\tilde{w}^{\dot{a}}_P(\tilde{\mathbf{u}}_{\hat{1}} + \tilde{\mathbf{u}}_2) - \tilde{u}^{\dot{a}}_P(\tilde{\mathbf{w}}_{\hat{1}} + \tilde{\mathbf{w}}_2)\,,
\end{aligned} \tag{5.18}$$

with the understanding that we are free to replace $\mathbf{u}_{\hat{1}} \leftrightarrow \mathbf{u}_2$ and $\tilde{\mathbf{u}}_{\hat{1}} \leftrightarrow \tilde{\mathbf{u}}_2$ at any step.

In practice, it is much easier to deal with supermomenta q_i than the u and w variables. It is straightforward to demonstrate that eq. (5.18) implies the substitutions,

$$q^A_P = -q^A_{\hat{1}} - q^A_2\,, \qquad\qquad \tilde{q}_{PA} = -\tilde{q}_{\hat{1}A} - \tilde{q}_{2A}\,. \tag{5.19}$$

Thus one can substitute the result for q_P in the tree amplitude on the right, avoiding the more complicated eq. (5.18), and extract out the full supermomentum-conservation delta function. At this stage, we are left with the task of integrating,

$$\delta^4\Big(\sum_{i\in\mathcal{E}} q_i^A\Big)\delta^4\Big(\sum_{i\in\mathcal{E}}\tilde{q}_{iB}\Big)q^{n-5}\tilde{q}^{n-5}\int d^2\eta_P d^2\tilde{\eta}_P \mathcal{A}_{3L}\,, \tag{5.20}$$

where the two delta functions correspond to the overall supermomentum conservation, and $\mathcal{E}$ is the set of all external legs of the full amplitude. The remaining integral has the solution,

$$\int d^2\eta_P d^2\tilde{\eta}_P \mathcal{A}_{3L} = i(\mathbf{u}_{\hat{1}} - \mathbf{u}_2)(\tilde{\mathbf{u}}_{\hat{1}} - \tilde{\mathbf{u}}_2)\,, \tag{5.21}$$

which can be re-written in terms of the $q, \tilde{q}$ as,

$$i\bigg(-\frac{q_{\hat{1}}\not{p}_K\not{p}_2\tilde{q}_{\hat{1}}}{s_{\hat{1}K}} - q_{\hat{1}}\tilde{q}_2 + q_2\tilde{q}_{\hat{1}} + \frac{q_2\not{p}_K\not{p}_{\hat{1}}\tilde{q}_2}{s_{2K}}\bigg)\,, \tag{5.22}$$

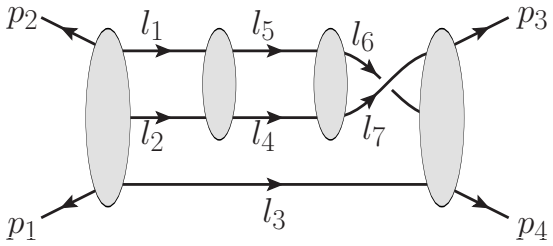

FIG. 4: A sample cut of the four-loop four-point amplitude.

where p_K is an arbitrary null reference vector. The sewing of a three-point amplitude with a general tree amplitude will thus result in the form,

$$\delta^4\Big(\sum_{i\in\mathcal{E}} q_i^A\Big)\delta^4\Big(\sum_{i\in\mathcal{E}} \tilde{q}_{iB}\Big) q^{n-5}\tilde{q}^{n-5}\Big(-\frac{q_{\hat{1}}\not{p}_K\not{p}_2\tilde{q}_{\hat{1}}}{s_{\hat{1}K}} - q_{\hat{1}}\tilde{q}_2 + q_2\tilde{q}_{\hat{1}} + \frac{q_2\not{p}_K\not{p}_{\hat{1}}\tilde{q}_2}{s_{2K}}\Big)\,, \tag{5.23}$$

where all $q, \tilde{q}$s are in terms of external lines and $q_{\hat{1}}$ is the shifted q_1 with z taking on the value at the pole.

Case (B):

For the case with no three-point subamplitudes, illustrated in fig. 3(B), we can always eliminate q_P and $\tilde{q}_P$ from the "R" amplitude, using the "L" delta functions. The Grassmann integral will then be of the form,

$$\delta^4\Big(\sum_{i\in\mathcal{E}} q_i^A\Big)\delta^4\Big(\sum_{i\in\mathcal{E}} \tilde{q}_{iB}\Big) f(q,\tilde{q}) \int d^2\eta_P d^2\tilde{\eta}_P\, \delta^4\Big(\sum_{i\in L} q_i^C\Big)\delta^4\Big(\sum_{i\in L} \tilde{q}_{iD}\Big)\,. \tag{5.24}$$

Focusing on the chiral integral, we proceed by splitting the delta function using eq. (5.12) on legs j and P, which gives,

$$\begin{aligned}
\int d^2\eta_P \delta^4\Big(\sum_{i\in L} q_i^C\Big) &= s_{jP}\,\delta^2\Big(\eta_{ja} + s_{jP}^{-1}\langle j_a|\not{P}(q_{\hat{1}} + \ldots + q_{j-1})\Big) \\
&= s_{jP}\,\delta^2\Big(s_{jP}^{-1}\langle j_a|\not{P}(q_{\hat{1}} + \ldots + q_j)\Big) \\
&= -s_{jP}^{-1}(q_{\hat{1}} + \ldots + q_j)\not{P}\not{p}_j\not{P}(q_{\hat{1}} + \ldots + q_j) \\
&= (q_{\hat{1}} + \ldots + q_j)^A(p_{\hat{1}} + \ldots + p_j)_{AB}(q_{\hat{1}} + \ldots + q_j)^B\,,
\end{aligned} \tag{5.25}$$

where $P = p_{\hat{1}} + p_2 + \cdots + p_j$, and we used the identity (5.9) between the first and second lines. Likewise, the antichiral integration contributes,

$$\int d^2\tilde{\eta}_P \delta^4\Big(\sum_{i\in L} \tilde{q}_{iD}\Big) = (\tilde{q}_{\hat{1}} + \ldots + \tilde{q}_j)_A(p_{\hat{1}} + \ldots + p_j)^{AB}(\tilde{q}_{\hat{1}} + \ldots + \tilde{q}_j)_B\,. \tag{5.26}$$

VI. MULTILOOP APPLICATIONS WITH MAXIMAL SUPERSYMMETRY

In this section we consider the construction of multiloop amplitudes in maximally supersymmetric Yang-Mills in six dimensions. We consider the $(1,1)$ theory, which, under a dimensional reduction to four dimensions, is equivalent to $\mathcal{N}=4$ sYM theory. After some general comments, we turn to a two-loop warmup before discussing four-point amplitudes at four and six loops.

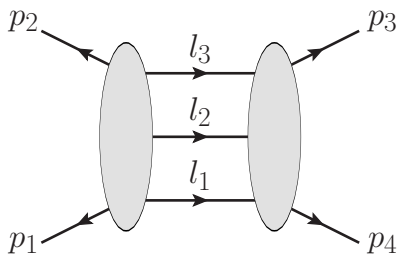

FIG. 5: The three-particle cut of a two-loop four-point amplitude.

A. General considerations

In unitarity cuts, one must sum over states in multiple lines. The supersum then corresponds to integrating over the $\eta, \tilde{\eta}$ coordinates of these lines. For example, when sewing the four-loop cut displayed in fig. 4, the sum over states is implemented by the Grassmann integration,

$$\int \prod_{i=1}^{7} \left(d^2\eta_{l_i} d^2\tilde{\eta}_{l_i} \right) \mathcal{A}_5^{(1)} \mathcal{A}_4^{(2)} \mathcal{A}_4^{(3)} \mathcal{A}_5^{(4)} \,, \tag{6.1}$$

where the superscript $\mathcal{A}_4^{(j)}$ labels the four distinct tree amplitudes composing the cut.

The strategy for dealing with such supersums is similar to the strategy used at tree level; we use eq. (5.12) to localize as many η integrals as possible. In cuts with no three-point subamplitudes, such as the cut in fig. 4, there is a supermomentum delta function on each tree amplitude. Each delta function can be used to localize two pairs of $\eta_l, \tilde{\eta}_l$ via eq. (5.12); in a cut with m tree amplitudes, a total of $2(m-1)$ pair of $\eta_l, \tilde{\eta}_l$ can be localized in this manner, with one overall $\delta^4(\sum_{\mathcal{E}} q)\delta^4(\sum_{\mathcal{E}} \tilde{q})$ extracted outside of the integral. We note that when solving the delta-function constraints, care must be taken to avoid circular solutions.

In general, the fermionic delta functions will be insufficient to localize all of the η integrals; the remaining integrals must be handled in a different manner. One approach is to expand the left-over integrand as a polynomial in $\eta_{l_i}, \tilde{\eta}_{l_i}$ and interpret the fermionic integral as instructions to pick out the coefficient of $\prod_i (\eta_{l_i})^2 (\tilde{\eta}_{l_i})^2$. We will apply this approach to a two-loop example in the next subsection.

Cuts that have three-point subamplitudes are generally more difficult, and may need to be handled on an *ad hoc* basis. One can usually make progress by combining three-point subamplitudes into higher-point amplitudes, as was done in the non-supersymmetric case in section IV. One can perform the remaining η integrals as before.

We note that for four-point loop amplitudes, after extracting out the overall supermomentum delta functions, the number of remaining $\eta, \tilde{\eta}$s will always match the number of Grassmann integrations. Therefore, the four-point loop amplitudes will depend on $\eta, \tilde{\eta}$ only through the supermomentum delta functions, i.e. they will be proportional to a four-point tree superamplitude.

To illustrate these techniques we now work out a few examples. (The cut of fig. 4 is evaluated in some detail in appendix A.)

B. Two-loop four-point example

We first evaluate the three-particle cut illustrated in fig. 5. The cut is given by sewing together two five-point tree superamplitudes,

$$C^{\text{2-loop}} = \int \prod_{i=1}^{3} d^2\eta_{l_i} d^2\tilde{\eta}_{l_i} \, \mathcal{A}_{5L}^{\text{tree}}(p_1, p_2, l_3, l_2, l_1) \mathcal{A}_{5R}^{\text{tree}}(p_3, p_4, -l_1, -l_2, -l_3) \,. \tag{6.2}$$

We choose the following convenient representations for the five-point tree superamplitudes:

$$\begin{aligned}
\mathcal{A}_{5L}^{\text{tree}} &= i\,\frac{\delta^4(\sum_L q)\delta^4(\sum_L \tilde{q})}{s_{l_3l_2}s_{l_2l_1}s_{l_11}s_{12}s_{2l_3}}\Big\{q_{l_3}^A(l_2l_1p_1p_2)_A{}^B\tilde{q}_{l_3B}+\text{cyclic}\\
&\quad+\frac{1}{2}\left[q_{l_3}^A\tilde{\Delta}_{l_2A}^L+q_{l_1}^A\tilde{\Delta}_{1A}^L+(q_{l_1}+q_1)^A\tilde{\Delta}_{2A}^L+(\text{chiral conjugate})\right]\Big\},\\
\mathcal{A}_{5R}^{\text{tree}} &= i\,\frac{\delta^4(\sum_R q)\delta^4(\sum_R \tilde{q})}{s_{l_1l_2}s_{l_2l_3}s_{l_33}s_{34}s_{4l_1}}\Big\{q_{l_1}^A(l_2l_3p_3p_4)_A{}^B\tilde{q}_{l_1B}+\text{cyclic}\\
&\quad+\frac{1}{2}\left[-q_{l_1}^A\tilde{\Delta}_{(-l_2)A}^R-q_{l_3}^A\tilde{\Delta}_{3A}^R+(q_3-q_{l_3})^A\tilde{\Delta}_{4A}^R+(\text{chiral conjugate})\right]\Big\},
\end{aligned}\tag{6.3}$$

where the L, R superscript of the Δ's denote with respect to which side of the cut they are defined. For example, we have,

$$\begin{aligned}
\tilde{\Delta}_{l_2A}^L &= (l_2l_1p_1p_2-l_2p_2p_1l_1)_A{}^B\tilde{q}_{l_2B}\,,\\
\tilde{\Delta}_{(-l_2)A}^R &= -(l_2l_3p_3p_4-l_2p_4p_3l_3)_A{}^B\tilde{q}_{l_2B}\,.
\end{aligned}\tag{6.4}$$

As discussed previously, one can extract an overall supermomentum delta function $\delta^4(\sum_{\mathcal{E}} q)\delta^4(\sum_{\mathcal{E}} \tilde{q})$ outside of the integral, leaving behind a degree eight delta function, which can be used to localize two pairs of ηs and $\tilde{\eta}$s. Here we choose to localize η_{l_1}, η_{l_2} and their antichiral partners. Thus the fermionic delta functions from the two tree amplitudes combine to give,

$$\begin{aligned}
&\delta^4\Big(\sum_L q\Big)\delta^4\Big(\sum_L \tilde{q}\Big)\delta^4\Big(\sum_R q\Big)\delta^4\Big(\sum_R \tilde{q}\Big)\\
&\quad= \delta^4\Big(\sum_{\mathcal{E}} q\Big)\delta^4\Big(\sum_{\mathcal{E}} \tilde{q}\Big)s_{l_1l_2}^2\\
&\qquad\times\delta^2\Big(\eta_{l_1a}+s_{l_1l_2}^{-1}\langle l_{1a}|\not{l}_2(q_{l_3}+q_1+q_2)\Big)\delta^2\Big(\eta_{l_2b}+s_{l_1l_2}^{-1}\langle l_{2b}|\not{l}_1(q_{l_3}+q_1+q_2)\Big)\\
&\qquad\times\delta^2\Big(\tilde{\eta}_{l_1}^{\dot{a}}+s_{l_1l_2}^{-1}[l_1^{\dot{a}}|\not{l}_2(\tilde{q}_{l_3}+\tilde{q}_1+\tilde{q}_2)\Big)\delta^2\Big(\tilde{\eta}_{l_2}^{\dot{b}}+s_{l_1l_2}^{-1}[l_2^{\dot{b}}|\not{l}_1(\tilde{q}_{l_3}+\tilde{q}_1+\tilde{q}_2)\Big)\,,
\end{aligned}\tag{6.5}$$

which is a direct application of eq. (5.12). From the above, one can immediately see that the delta function localizes the $d^2\eta_{l_i}d^2\tilde{\eta}_{l_i}$ integral in eq. (6.2) for $i=1,2$.

After factoring out the fermionic delta functions in $\mathcal{A}_{5L}\mathcal{A}_{5R}$, the remaining function is of Grassmann degree four, and only terms proportional to $(\eta_{l_3})^2(\tilde{\eta}_{l_3})^2$ can saturate the remaining Grassmann integrals. Keeping in mind that $\eta_{l_1},\eta_{l_2},\tilde{\eta}_{l_1},\tilde{\eta}_{l_2}$ are localized through eq. (6.5), the contributing terms in the curly bracket in eq. (6.3) are,

$$\begin{aligned}
&\Big\{q_{l_3}^A(l_2l_1p_1p_2)_A{}^B\tilde{q}_{l_3B}+q_{l_2}^A(l_1p_1p_2l_3)_A{}^B\tilde{q}_{l_2B}+q_{l_1}^A(p_1p_2l_3l_2)_A{}^B\tilde{q}_{l_1B}+\frac{1}{2}\left[q_{l_3}^A\tilde{\Delta}_{l_2A}^L+\tilde{q}_{l_3A}\Delta_{l_2}^{LA}\right]\Big\}\\
&\times\Big\{q_{l_1}^A(l_2l_3p_3p_4)_A{}^B\tilde{q}_{l_1B}+q_{l_2}^A(l_3p_3p_4l_1)_A{}^B\tilde{q}_{l_2B}+q_{l_3}^A(p_3p_4l_1l_2)_A{}^B\tilde{q}_{l_3B}-\frac{1}{2}\left[q_{l_1}^A\tilde{\Delta}_{(-l_2)A}^R+\tilde{q}_{l_1A}\Delta_{(-l_2)}^{RA}\right]\Big\}.
\end{aligned}\tag{6.6}$$

Thus performing the final $d^2\eta_{l_3}d^2\tilde{\eta}_{l_3}$ integration gives for eq. (6.2),

$$\begin{aligned}
C^{\text{2-loop}} &= \frac{is_{23}\mathcal{A}_4^{\text{tree}}(p_1,p_2,p_3,p_4)}{s_{12}(l_3+l_2)^4(l_1+p_1)^2(p_2+l_3)^2(l_3-p_3)^2(p_4-l_1)^2}\\
&\quad\times\Big\{\langle l_3|\not{l}_2\not{l}_1\not{p}_1\not{p}_2+\frac{\not{l}_1\not{p}_1\not{p}_2\not{l}_3\not{l}_2\not{l}_1}{(l_1+l_2)^2}+\frac{\not{l}_2\not{l}_1\not{p}_1\not{p}_2\not{l}_3\not{l}_2}{(l_1+l_2)^2}|l_3]\\
&\qquad-\frac{1}{2}\left[\langle l_3|\frac{(\not{l}_2\not{l}_1\not{p}_1\not{p}_2-\not{l}_2\not{p}_2\not{p}_1\not{l}_1)\not{l}_2\not{l}_1}{(l_1+l_2)^2}|l_3]-[l_3|\frac{(\not{l}_2\not{l}_1\not{p}_1\not{p}_2-\not{l}_2\not{p}_2\not{p}_1\not{l}_1)\not{l}_2\not{l}_1}{(l_1+l_2)^2}|l_3\rangle\right]\Big\}_{\dot{a}}^{a}\\
&\quad\times\Big\{\langle l_3|\frac{\not{l}_2\not{l}_3\not{p}_3\not{p}_4\not{l}_1\not{l}_2}{(l_1+l_2)^2}+\frac{\not{l}_1\not{l}_2\not{l}_3\not{p}_3\not{p}_4\not{l}_1}{(l_1+l_2)^2}+\not{p}_3\not{p}_4\not{l}_1\not{l}_2|l_3]\\
&\qquad+\frac{1}{2}\left[\langle l_3|\frac{(\not{l}_2\not{l}_3\not{p}_3\not{p}_4-\not{l}_2\not{p}_4\not{p}_3\not{l}_3)\not{l}_2\not{l}_1}{(l_1+l_2)^2}|l_3]-[l_3|\frac{(\not{l}_2\not{l}_3\not{p}_3\not{p}_4-\not{l}_2\not{p}_4\not{p}_3\not{l}_3)\not{l}_2\not{l}_1}{(l_1+l_2)^2}|l_3\rangle\right]\Big\}_{a}^{\dot{a}}.
\end{aligned}\tag{6.7}$$

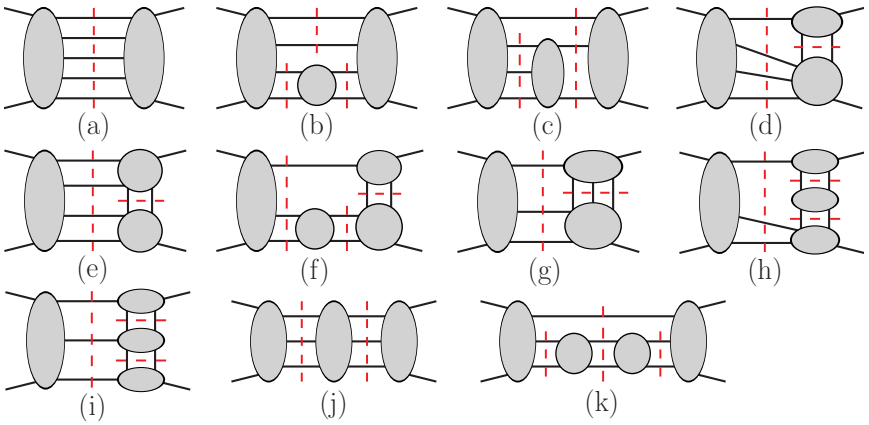

FIG. 6: The eleven basic cuts decomposing a four-point four-loop amplitude into a product of tree amplitudes. Together with ones involving two-particle cuts, these are the basic ones for determining a massless four-point four-loop amplitude, including nonplanar contributions [18, 47]. The complete spanning set is given by taking all possible distinct permutations of cut and external legs.

This expression can be cleaned up further, but for our purposes it is simplest to numerically evaluate it. We have numerically checked that after dividing by the tree amplitude, this expression matches the analogous expression obtained using four-dimensional cuts [46, 49], but extended into six dimensions. Since the four-dimensional expression depends only on Lorentz dot products of momenta, this extension is carried out simply by treating the dot products as six-dimensional ones.

C. Multiloop $\mathcal{N} = 4$ super-Yang-Mills and $\mathcal{N} = 8$ supergravity

Following the procedure described above, one can directly check the six-dimensional unitarity cuts of more complicated multiloop $\mathcal{N} = 4$ sYM amplitudes. Up to three loops, the four-gluon amplitude is known to be valid in D dimensions (subject to mild power counting assumptions) [16, 17]. As a nontrivial application of the methods described above, here we confirm that the complete four-loop four-particle amplitudes of $\mathcal{N} = 4$ sYM theory computed in ref. [47] are indeed valid for $D \leq 6$. In that paper, the amplitude was given as a linear combination of 50 integrals of the form,

$$stA_4^{\text{tree}} \int \left(\prod_{i=1}^{4} \frac{d^D l_i}{(2\pi)^D} \right) \frac{N_k(l_i, p_i)}{\prod_{j=1}^{16} l_j^2}, \tag{6.8}$$

where the numerator N_k is a polynomial of degree six in the loop and external momenta. Of these integrals, six are planar and the rest nonplanar. In ref. [47], many of the terms in the numerators were explicitly determined using cuts with $D = 4$ momenta and helicity states. Although a number of nontrivial checks were performed partially confirming their validity in $D > 4$ dimensions, it is still useful to have a complete confirmation valid especially for $D = 11/2$, which is the lowest dimension where an ultraviolet divergence can occur.

As explained in ref. [18], the validity of $\mathcal{N} = 4$ sYM amplitudes in D dimensions implies that the corresponding $\mathcal{N} = 8$ supergravity amplitudes are valid as well. This follows from the construction of $\mathcal{N} = 8$ supergravity amplitudes from corresponding $\mathcal{N} = 4$ sYM amplitudes using the unitarity method in conjunction with the KLT relations [57], which are known to be valid in D dimensions. We therefore need only confirm the $D = 6$ validity of the $\mathcal{N} = 4$ sYM amplitudes to confirm the result for $\mathcal{N} = 8$ supergravity for $4 < D \leq 6$. A key conclusion of ref. [18] is that the four-loop four-point amplitude of $\mathcal{N} = 8$ supergravity then cannot diverge in dimensions lower than $D = 11/2$, matching the behavior of $\mathcal{N} = 4$ sYM theory.

As discussed in refs. [18, 47], any four-point four-loop amplitude of a massless theory can be completely determined (up to scale-free integrals that integrate to zero in dimensional regularization) via a set of eleven basic cuts shown in fig. 6 along with simpler ones containing two-particle cuts, not displayed. The complete spanning set is obtained by considering all permutations of the legs of each constituent tree amplitude. This set is constructed by demanding that

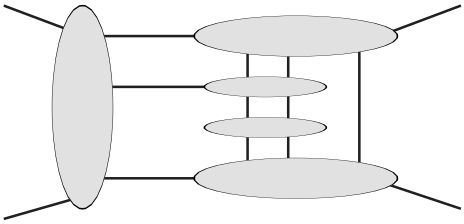

FIG. 7: A nontrivial cut of the planar four-point six-loop $\mathcal{N} = 4$ sYM theory.

all potential terms are detectable in at least one cut. To carry out our six-dimensional evaluation, we compare the cuts formed from the products of tree amplitudes against the corresponding cuts of the amplitudes as given in ref. [47]. In the latter form, after dividing by the tree amplitude, only Lorentz inner products remain in the amplitude, making numerical comparisons in six dimensions straightforward. In appendix A, we give an explicit analytic evaluation of the sample nonplanar cut shown in fig. 4.

More generally, after extracting an overall supermomentum-conservation delta function from the cuts, the remaining delta functions localize most of the $\eta\tilde{\eta}$ integration, leaving behind six, four, and two pairs of $\eta\tilde{\eta}$ respectively for diagrams (a), (b,c,d,e,g,j), and (f,h,i,k). These extra pairs of $\eta\tilde{\eta}$s then saturate the remaining integration, as was the case in the two-loop example above. This then gives us a result for the state sum of these cuts, which we evaluate with six-dimensional kinematics constrained to satisfy the on-shell conditions.

We find appropriate numerical solutions to the cut conditions by sequentially building momenta that satisfy the on-shell conditions of each of the constituent tree amplitudes in a cut. For a constituent n-point tree amplitude, we need to impose momentum conservation and take the momenta on shell, $p_i^2 = 0$. For $n-2$ of the legs, we can choose arbitrary null vectors, imposing the momentum conservation constraints on the final two legs. We label the sum of the arbitrary $n-2$ momenta as $P = \sum_i^{n-2} p_i$. We then define $p_{n-1} \equiv \left(-P^2/2k \cdot P\right) k$, where k is an arbitrary null vector. With this choice then $p_n \equiv p_{n-1} + K$ automatically satisfies the on-shell condition $p_n^2 = 0$. (It can happen that momentum conservation constraints can lead to inconsistencies in this simple procedure, if a tree does not have at least two unspecified legs. Although this can always be avoided in our case, we note that such inconsistencies can be resolved by solving the cut conditions for groups of tree amplitudes instead of one by one.)

By systematically stepping through the spanning set of cuts described above, we confirm that for $D \leq 6$ the full amplitude is correctly constructed by the mostly four-dimensional evaluation of ref. [47], as expected.

Another interesting case is the four-point six-loop amplitude of $\mathcal{N} = 4$ sYM theory. At six loops, the planar amplitudes can be expressed as a linear combination of integrals similar to the four-loop form (6.8) [58], except that the numerator N_k is a polynomial in the loop and external momenta of degree ten instead of degree six. In four dimensions, any Gram determinant $\det(p_i \cdot p_j)$ vanishes for p_i and p_j corresponding to any five independent momenta, since there can be no more than four linearly independent momenta. For the six-loop four-point amplitude we have a total of nine independent external and loop momenta. Thus with four-dimensional momenta and spinors in the cuts, the constructed amplitude is trivially invariant under the shifts,

$$N_m \to N_m + a_m \det(p_i \cdot p_j)\,, \tag{6.9}$$

although its form changes. The a_m are constants. If we impose dual conformal symmetry [7–9, 12], the planar numerators are fixed with $a_m = 0$. What about higher dimensions? Iterated two-particle cuts are simple to evaluate in D dimensions [46, 49], with the result that all a_m detectable in such cuts vanish. As a more nontrivial check, we evaluated the cut shown in fig. 7 in six dimensions using the methods described above and numerically compared it against the same cut obtained via four-dimensional methods [12, 38, 47] and extended into six dimensions. Because this cut is composed of four- and five-point tree amplitudes, its evaluation in six dimensions is similar to the four-loop cut described in appendix A. We find that $a_m = 0$ in six dimensions to match the cut fig. 7. Although we did not check a spanning set of cuts, this result strongly suggests that all a_m vanish.

VII. DUAL CONFORMAL PROPERTIES IN HIGHER DIMENSIONS

The above results suggest that integrands of $\mathcal{N} = 4$ sYM evaluated in six dimensions should have simple dual conformal properties. If this were to hold, it would lead to important restrictions on the form of the integrands,

guiding their construction in six dimensions, or equivalently in four dimensions but with masses.

In four dimensions, the dual conformal boost generators are [9],

$$K^\mu = \sum_{i=1}^{n} \left[2x_i^\mu x_i^\nu \frac{\partial}{\partial x_i^\nu} - x_i^2 \frac{\partial}{\partial x_{i\mu}} \right] , \tag{7.1}$$

where $\mu = 0, 1, 2, 3$, and the dual coordinates x are defined via,

$$x_{i,i+1} = x_i^\mu - x_{i+1}^\mu = p_i^\mu \, . \tag{7.2}$$

The principal constraint on amplitudes comes from the inversion symmetry $x_i^\mu \to x_{i\mu}/x_i^2$. Since the integrals are all dual translational invariant, they will also be dual conformal boost invariant as long as they are invariant under inversion. This is because the conformal boost is a combination of translations and inversions. Under the inversion, we have,

$$x_{ij}^2 \to \frac{x_{ij}^2}{x_i^2 x_j^2} \, , \qquad d^4 x_i \to \frac{d^4 x_i}{x_i^8} \, . \tag{7.3}$$

We can extend this to six dimensions by adding extra terms to the generator, which in SO(1,3)×SO(2) notation, is

$$\hat{K}^\mu = K^\mu + \sum_{i=1}^{n} \left[2x_i^\mu \left(n_i \frac{\partial}{\partial n_i} + \tilde{n}_i \frac{\partial}{\partial \tilde{n}_i} \right) + (n_i^2 + \tilde{n}_i^2) \frac{\partial}{\partial x_{i\mu}} \right] , \tag{7.4}$$

where we explicitly include the sign from our choice of metric in the extra-dimensional components. The extra-dimensional dual variables are

$$n_i - n_{i+1} = p_i^4 \, , \qquad \tilde{n}_i - \tilde{n}_{i+1} = p_i^5 \, .$$

This modification of the dual conformal generators is chosen so that the integrands maintain the same dual conformal weight as in four dimensions. On the other hand, the integration measure does depend on the dimension,

$$d^4 x_i \to \frac{d^4 x_i}{\hat{x}_i^8} \, , \qquad dn_i \to \frac{dn_i}{\hat{x}_i^2} \, , \qquad d\tilde{n}_i \to \frac{d\tilde{n}_i}{\hat{x}_i^2} \, , \qquad d^6 \hat{x}_i \to \frac{d^6 \hat{x}_i}{\hat{x}_i^{12}} \, , \tag{7.5}$$

where here the hats denote six-dimensional quantities, with $\hat{x}_i^2 = x_i^2 - n_i^2 - \tilde{n}_i^2$. To maintain the invariance of the amplitude, we therefore should truncate the integration to four dimensions, which is equivalent to treating the extra-dimensional components as fixed masses. Of course, even if we choose to integrate over the extra dimensions, the fact that the integrands transform with a definite dual conformal weight puts severe restrictions on their form. The SO(1,3)×SO(2) decomposition is especially convenient for treating the amplitudes as four-dimensional but containing mass parameters, using the decomposition (2.17) of six-dimensional spinors into four-dimensional ones. This extension of dual conformal properties to higher dimensions is thus related to the extension for the Higgs regulated case [48].

Note that eq. (7.4) gives simply the first four components of the six-dimensional dual conformal boost generator. The observed form invariance of the four-point integrands (after dividing out the tree amplitude) suggests that we can treat the generator in a fully covariant form, similar to eq. (7.1), except we allow the indices μ and ν to run over all six components.

Furthermore, we note that the dual conformal boost generator can also be defined on the spinor variables. We start with the form of the dual conformal boost generator defined on the dual coordinates, and modify it to act also on spinors and to preserve the constraint equations that define the dual coordinates,

$$\begin{aligned} (x_i - x_{i+1})^{AB} &= p_i^{AB} = \lambda_i^{Aa} \lambda_{ia}^B \, , \\ (x_i - x_{i+1})_{AB} &= p_{iAB} = \tilde{\lambda}_{iA\dot{a}} \tilde{\lambda}_{iB}^{\dot{a}} \, . \end{aligned} \tag{7.6}$$

This gives the generator in the full space $(\lambda, \tilde{\lambda}, x)$,

$$\begin{aligned} \hat{K}^\mu \;=\; \sum_{j=1}^{n} \Bigg[& 2\hat{x}_j^\mu \hat{x}_j^\nu \frac{\partial}{\partial \hat{x}_j^\nu} - \hat{x}_j^2 \frac{\partial}{\partial \hat{x}_{j\mu}} + \frac{1}{2} \lambda_{ja}^A (\sigma^\mu)_{AB} (\hat{x}_j + \hat{x}_{j+1})^{BC} \frac{\partial}{\partial \lambda_{ja}^C} \\ & + \frac{1}{2} \tilde{\lambda}_{jA\dot{a}} (\tilde{\sigma}^\mu)^{AB} (\hat{x}_j + \hat{x}_{j+1})_{BC} \frac{\partial}{\partial \tilde{\lambda}_{jC\dot{a}}} \Bigg] . \end{aligned} \tag{7.7}$$

As in $D = 4$, we expect the dual conformal properties to be more transparent for superamplitudes rather than ordinary amplitudes [36]. It is not difficult to check that the four-point tree superamplitude transforms covariantly under a six-dimensional extension of dual conformal transformations. Introducing the dual superspace coordinates,

$$\theta_i^A - \theta_{i+1}^A = \lambda_i^{Aa}\eta_{ia} = q_i^A\,, \qquad \tilde{\theta}_{iA} - \tilde{\theta}_{i+1A} = \tilde{\lambda}_{iA\dot{a}}\tilde{\eta}_i^{\dot{a}} = \tilde{q}_{iA}\,, \tag{7.8}$$

the four-point tree-level superamplitude in dual superspace is

$$\mathcal{A}_4^{\rm tree} = -i\frac{\delta^6(\hat{x}_1 - \hat{x}_5)\delta^4(\theta_1 - \theta_5)\delta^4(\tilde{\theta}_1 - \tilde{\theta}_5)}{\hat{x}_{13}^2\hat{x}_{24}^2}. \tag{7.9}$$

Using the usual dual conformal-inversion properties of the supercoordinates,

$$\theta_i^A \to \frac{\hat{x}_{iAB}}{\hat{x}_i^2}\theta_i^B\,, \qquad \tilde{\theta}_{iA} \to \frac{\hat{x}_i^{AB}}{\hat{x}_i^2}\tilde{\theta}_{iB}, \tag{7.10}$$

the four-point amplitude transforms as,

$$\mathcal{A}_4^{\rm tree} \to (\hat{x}_1^2)^2(\hat{x}_1^2\hat{x}_2^2\hat{x}_3^2\hat{x}_4^2)\mathcal{A}_4^{\rm tree}\,. \tag{7.11}$$

The extra weight on $\hat{x}_1$ is due to the delta functions, which choose a specific point to enforce the cyclic identification.

It would of course be interesting to further study the implications of dual conformal transformations on higher-dimensional integrands, especially at higher points. For example, one can show using BCFW recursion that under dual conformal inversions for $n \geq 4$, the six-dimensional superamplitudes behave as [59],

$$\mathcal{A}_n^{\rm tree} \to (\hat{x}_1^2)^2\Big(\prod_{i=1}^n \hat{x}_i^2\Big)\mathcal{A}_n^{\rm tree}\,, \tag{7.12}$$

where $\hat{x}_1$ is the special point taken to enforce momentum conservation in the dual space.

VIII. COMMENTS AND CONCLUSIONS

In this paper, we developed six-dimensional helicity [34] as a practical tool in unitarity-based calculations of loop amplitudes. As simple illustrations we described the unitarity cuts of one-loop four-point amplitudes in QCD. As more sophisticated examples, we also described multiloop amplitudes in $\mathcal{N} = 4$ sYM theory, using also the DHS on-shell superspace [43]. To illustrate this, we worked out the three-particle cut of a two-loop four-point amplitude in some detail, before turning to higher-loop cases. Our results confirm that the four-loop four-point $\mathcal{N} = 4$ sYM and $\mathcal{N} = 8$ supergravity amplitudes obtained in refs. [18, 47] using mainly four-dimensional techniques are complete for $D \leq 6$, as expected.

There are a number of obvious further applications and studies that would be interesting to carry out. Our six-dimensional approach can be reinterpreted as a massive approach, by expressing six-dimensional spinors and momenta in terms of four-dimensional quantities, with the extra-dimensional pieces interpreted as mass terms. For one-loop QCD amplitudes, this should give forms of the cuts similar to the massive approach for rational terms taken by Badger [31]. It would be interesting to make the connection precise. More generally, it would, of course, be interesting to apply the unitarity-based six-dimensional helicity method described here to cases of phenomenological interest in QCD and to compare them to other approaches.

In general, the integrands of amplitudes can contain terms that vanish when loop momenta are set to $D = 4$, but are nonvanishing in higher dimensions. This can make it dangerous to extrapolate results from cuts in four dimensions to higher dimensions. Similarly, in a massive infrared regularization scheme [48], or when studying the Coulomb branch of gauge theories, additional mass terms can be present. The six-dimensional helicity formalism is well suited for systematically deriving such terms via unitarity. Interesting cases are two-loop $\mathcal{N} = 4$ amplitudes at six and higher points where we know such additional terms can appear [14]. Even at four points, the power counting in this theory is such that starting at six loops contributions proportional to Gram determinants that vanish in four dimensions but are non-vanishing in higher dimensions in principle can appear, though our results indicate that they do not. The six-dimensional formalism may also shed light on the peculiar pattern of vanishing and non-vanishing integral coefficients in MHV and non-MHV amplitudes at higher points in the $\mathcal{N} = 4$ theory [60], because six-dimensional helicity treats these cases in a unified way. In principle, it would be worthwhile to evaluate cuts using even higher

dimensions, but six-dimensional methods push any potential lost terms to rather large numbers of loops or legs. For example, covariance and simple power counting considerations suggest that four-point amplitudes in $\mathcal{N} = 4$ sYM theory will be free of terms that can vanish in six dimensions through at least eight loops.

We noted that the expressions for the four-point planar integrands through at least six loops do not appear to differ between four and six dimensions. This suggests that the integrands of amplitudes in higher dimensions will also be constrained by extensions of dual conformal symmetry. Based on this, we proposed a six-dimensional extension of the dual conformal symmetry generators. We also noted that the four-point tree amplitudes of $\mathcal{N} = 4$ sYM theory have simple properties under this extension, and proposed the general property at n points [59]. Our six-dimensional extension is connected to a recently proposed extension of the dual conformal generators to massive amplitudes [48]. It is also likely connected to a ten-dimensional extension [61]. More generally, it seems likely that extensions of the four-dimensional structures identified in planar loop integrands [15] will restrict the form in higher dimensions as well. The BCJ relations between planar and nonplanar contributions [4, 50] then suggest that nonplanar integrands will also be restricted by extensions of the four-dimensional structures. This warrants further study, especially for larger numbers of external legs.

In summary, six-dimensional helicity and its associated on-shell superspace are additional useful tools both for carrying out loop calculations in conjunction with the unitarity method and for uncovering new structures in scattering amplitudes.

Acknowledgments

We thank Lance Dixon, Michael Douglas, Johannes Henn, Henrik Johansson, Donal O'Connell, and especially Radu Roiban for many stimulating discussions. We thank Academic Technology Services at UCLA for computer support. This research was supported by the US Department of Energy under contract DE–FG03–91ER40662. J. J. M. C. gratefully acknowledges the Stanford Institute for Theoretical Physics for financial support. HI's work is supported by a grant from the US LHC Theory Initiative through NSF contract PHY–0705682.

Appendix A: An Analytic Four-Loop Cut

In this appendix, we present a nontrivial cut of the four-loop four-point amplitude of $\mathcal{N} = 4$ sYM. In particular, we analytically evaluate the cut shown in fig. 4, which is a nonplanar permutation of the cut (k) in fig. 6. Since this cut consists of only four- and five-point subamplitudes, the calculation is not significantly more difficult than the two-loop example in section VI B. The cut is evaluated by carrying out the Grassmann integration,

$$\begin{aligned} C^{\text{4-loop}} \;=\; & \int \Big(\prod_{i=1}^{7} d^2\eta_{l_i} d^2\tilde{\eta}_{l_i}\Big) \mathcal{A}_5^{\text{tree}}(p_1, p_2, l_1, l_2, l_3)\, \mathcal{A}_4^{\text{tree}}(-l_1, -l_2, l_4, l_5) \\ & \times \mathcal{A}_4^{\text{tree}}(-l_4, -l_5, l_6, l_7)\, \mathcal{A}_5^{\text{tree}}(p_3, p_4, -l_3, -l_6, -l_7)\,. \end{aligned} \tag{A1}$$

Here we have seven on-shell internal momenta labeled l_i, and four component tree amplitudes. In this cut, we can use the supermomentum delta functions to localize six of the seven internal supercoordinates $\eta_{l_i}, \tilde{\eta}_{l_i}$. The remaining supercoordinate integration is handled in the same way as in the example of section VI B.

A solution to the supercoordinate delta-function constraints is

$$\begin{aligned} q_{l_1} &\to -s_{l_1 l_2}^{-1} \not{l}_1 \not{l}_2 q_{l_3}\,, & \tilde{q}_{l_1} &\to -s_{l_1 l_1}^{-1} \not{l}_1 \not{l}_2 \tilde{q}_{l_3}\,, \\ q_{l_2} &\to -s_{l_1 l_2}^{-1} \not{l}_2 \not{l}_1 q_{l_3}\,, & \tilde{q}_{l_2} &\to -s_{l_1 l_2}^{-1} \not{l}_2 \not{l}_1 \tilde{q}_{l_3}\,, \\ q_{l_4} &\to -s_{l_4 l_5}^{-1} \not{l}_4 \not{l}_5 q_{l_3}\,, & \tilde{q}_{l_4} &\to -s_{l_4 l_5}^{-1} \not{l}_4 \not{l}_5 \tilde{q}_{l_3}\,, \\ q_{l_5} &\to -s_{l_4 l_5}^{-1} \not{l}_5 \not{l}_4 q_{l_3}\,, & \tilde{q}_{l_5} &\to -s_{l_4 l_5}^{-1} \not{l}_5 \not{l}_4 \tilde{q}_{l_3}\,, \\ q_{l_6} &\to -s_{l_6 l_7}^{-1} \not{l}_6 \not{l}_7 q_{l_3}\,, & \tilde{q}_{l_6} &\to -s_{l_6 l_7}^{-1} \not{l}_6 \not{l}_7 \tilde{q}_{l_3}\,, \\ q_{l_7} &\to -s_{l_6 l_7}^{-1} \not{l}_7 \not{l}_6 q_{l_3}\,, & \tilde{q}_{l_7} &\to -s_{l_6 l_7}^{-1} \not{l}_7 \not{l}_6 \tilde{q}_{l_3}\,, \end{aligned} \tag{A2}$$

where we have ignored all dependence on $\{q_1, q_2, q_3, q_4\}$, since these will drop out after the final η_{l_3} integration. As usual, we take the Mandelstam invariants to be $s_{l_i l_j} = (l_i + l_j)^2$. Because of extra factors of these invariants coming

from the Grassmann integrations — seen in eq. (6.5) — we must also multiply the final cut by $s^2_{l_1 l_2} s^2_{l_4 l_5} s^2_{l_6 l_7}$. The rest of the calculation is similar to the derivation of eq. (6.7), giving,

$$
\begin{aligned}
C^{\text{4-loop}} \;=\; & \frac{s_{23}(l_4+l_5)^2(l_6+l_7)^2 \mathcal{A}_4^{\text{tree}}(p_1,p_2,p_3,p_4)}{s_{12}(p_1+l_3)^2(p_2+l_1)^2(p_3-l_7)^2(p_4-l_3)^2(l_2+l_3)^2(l_2-l_4)^2(l_5-l_6)^2(l_3+l_6)^2} \\
& \times \langle l_3^a | \Bigg(\not{p}_1 \not{p}_2 \not{l}_1 \not{l}_2 + \frac{\not{l}_2 \not{l}_3 \not{p}_1 \not{p}_2 \not{l}_1 \not{l}_2 + \not{l}_1 \not{l}_2 \not{l}_3 \not{p}_1 \not{p}_2 \not{l}_1}{(l_1+l_2)^2} \\
& \quad - \frac{\not{l}_1 \not{l}_2 (\not{l}_3 \not{p}_1 \not{p}_2 \not{l}_1 - \not{l}_3 \not{l}_1 \not{p}_2 \not{p}_1) - (\not{l}_1 \not{p}_2 \not{p}_1 \not{l}_3 - \not{p}_1 \not{p}_2 \not{l}_1 \not{l}_3) \not{l}_2 \not{l}_1}{2(l_1+l_2)^2} \Bigg) | l_{3\dot{a}}] \\
& \times \langle l_{3a} | \Bigg(\not{l}_6 \not{l}_7 \not{p}_3 \not{p}_4 + \frac{\not{l}_7 \not{p}_3 \not{p}_4 \not{l}_3 \not{l}_6 \not{l}_7 + \not{l}_6 \not{l}_7 \not{p}_3 \not{p}_4 \not{l}_3 \not{l}_6}{(l_6+l_7)^2} \\
& \quad + \frac{(\not{l}_7 \not{p}_3 \not{p}_4 \not{l}_3 - \not{l}_7 \not{l}_3 \not{p}_4 \not{p}_3) \not{l}_7 \not{l}_6 - \not{l}_6 \not{l}_7 (\not{l}_3 \not{p}_4 \not{p}_3 \not{l}_7 - \not{p}_3 \not{p}_4 \not{l}_3 \not{l}_7)}{2(l_6+l_7)^2} \Bigg) | l_3^{\dot{a}}] \,.
\end{aligned}
\tag{A3}
$$

This expression is just a gamma trace, and although it appears to be chiral, the γ_7 term in the trace actually drops out. In fact, the five-point tree amplitude itself is non-chiral, although this property is not manifest in the present form.

One can compare this to the cut of the amplitude derived in ref. [47] using (mostly) four-dimensional methods,

$$
\begin{aligned}
C^{\text{4-loop}} \;=\; & \frac{s_{12} s_{23} \mathcal{A}_4^{\text{tree}}(p_1,p_2,p_3,p_4)}{(p_2+l_1)^2(p_3-l_7)^2(l_1-l_5)^2(l_4-l_7)^2} \\
& \times \Bigg(\frac{s_{12}^2 (l_2-l_6)^2}{(l_2+l_3)^2(l_3+l_6)^2} + \frac{s_{23}(l_4+l_5)^4}{(p_1+l_3)^2(p_4-l_3)^2} \\
& \quad + \frac{s_{12}(l_4+l_5)^2(p_1+l_3+l_6)^2}{(p_1+l_3)^2(l_3+l_6)^2} + \frac{s_{12}(l_4+l_5)^2(p_4-l_2-l_3)^2}{(p_4-l_3)^2(l_2+l_3)^2} \Bigg) \,.
\end{aligned}
\tag{A4}
$$

We have evaluated these two expressions numerically using six-dimensional momenta to verify their equality.

Appendix B: Auxiliary variables at three points

In this appendix, we summarize the construction of the variables needed to define the three-point amplitudes in eqs. (2.22) and (5.7), as given in ref. [34]. At three points, momentum conservation and on-shell conditions mean that the Lorentz products of the momenta all vanish. This gives a vanishing determinant of the Lorentz-invariant inner product of a fundamental and an anti-fundamental spinor, i.e. the 2×2 matrix $\langle i_a | j_{\dot{a}}]$ has rank one, so that $\langle i_a | j_{\dot{a}}] = u_{ia} \tilde{u}_{j\dot{a}}$. Consistently defining these SU(2) spinors for all Lorentz invariants, we have (for $\{i,j\}$ cyclically ordered),

$$
\langle i_a | j_{\dot{a}}] = u_{ia} \tilde{u}_{j\dot{a}} \,, \qquad\qquad \langle j_a | i_{\dot{a}}] = -u_{ja} \tilde{u}_{i\dot{a}} \,. \tag{B1}
$$

One important property of these SU(2) spinors can be derived from momentum conservation,

$$
u_1^c \langle 1_c | = u_2^c \langle 2_c | = u_3^c \langle 3_c | \,, \qquad\qquad \tilde{u}_{1\dot{c}} [1^{\dot{c}}| = \tilde{u}_{2\dot{c}} [2^{\dot{c}}| = \tilde{u}_{3\dot{c}} [3^{\dot{c}}| \,. \tag{B2}
$$

Ref. [34] also defines a pseudoinverse of these spinors,

$$
u_a w_b - u_b w_a = \epsilon_{ab} \,, \qquad\qquad \tilde{u}_{\dot{a}} \tilde{w}_{\dot{b}} - \tilde{u}_{\dot{b}} \tilde{w}_{\dot{a}} = \epsilon_{\dot{a}\dot{b}} \,, \tag{B3}
$$

subject to the additional condition,

$$
w_1^a \lambda_{1a}^A + w_2^a \lambda_{2a}^A + w_3^a \lambda_{3a}^A = 0 \,, \qquad\qquad \tilde{w}_{1\dot{a}} \tilde{\lambda}_{1A}^{\dot{a}} + \tilde{w}_{2\dot{a}} \tilde{\lambda}_{2A}^{\dot{a}} + \tilde{w}_{3\dot{a}} \tilde{\lambda}_{3A}^{\dot{a}} = 0 \,. \tag{B4}
$$

[1] Z. Bern, L. J. Dixon, D. C. Dunbar and D. A. Kosower, Nucl. Phys. B **425**, 217 (1994) [hep-ph/9403226]; Nucl. Phys. B **435**, 59 (1995) [hep-ph/9409265];
Z. Bern, L. J. Dixon and D. A. Kosower, Ann. Rev. Nucl. Part. Sci. **46**, 109 (1996) [hep-ph/9602280].

[2] R. Britto, F. Cachazo, B. Feng and E. Witten, Phys. Rev. Lett. **94**, 181602 (2005) [hep-th/0501052].

[3] E. Witten, Commun. Math. Phys. **252**, 189 (2004) [hep-th/0312171];
R. Roiban, M. Spradlin and A. Volovich, JHEP **0404**, 012 (2004) [hep-th/0402016]; Phys. Rev. D **70**, 026009 (2004) [hep-th/0403190].

[4] Z. Bern, J. J. M. Carrasco and H. Johansson, Phys. Rev. D **78**, 085011 (2008) [0805.3993 [hep-ph]].

[5] C. Anastasiou, Z. Bern, L. J. Dixon and D. A. Kosower, Phys. Rev. Lett. **91**, 251602 (2003) [hep-th/0309040];
Z. Bern, L. J. Dixon and V. A. Smirnov, Phys. Rev. D **72**, 085001 (2005) [hep-th/0505205].

[6] L. F. Alday and J. Maldacena, JHEP **0706**, 064 (2007) [0705.0303 [hep-th]].

[7] J. M. Drummond, J. Henn, V. A. Smirnov and E. Sokatchev, JHEP **0701**, 064 (2007) [hep-th/0607160];
A. Brandhuber, P. Heslop and G. Travaglini, Nucl. Phys. B **794**, 231 (2008) [0707.1153 [hep-th]].

[8] Z. Bern, M. Czakon, L. J. Dixon, D. A. Kosower and V. A. Smirnov, Phys. Rev. D **75**, 085010 (2007) [hep-th/0610248].

[9] J. M. Drummond, J. Henn, G. P. Korchemsky and E. Sokatchev, Nucl. Phys. B **795**, 52 (2008) [0709.2368 [hep-th]];
J. M. Drummond, J. Henn, G. P. Korchemsky and E. Sokatchev, Nucl. Phys. B **826**, 337 (2010) [0712.1223 [hep-th]].

[10] N. Arkani-Hamed, F. Cachazo, C. Cheung and J. Kaplan, JHEP **1003**, 020 (2010) [0907.5418 [hep-th]];
M. Bullimore, L. Mason and D. Skinner, JHEP **1003**, 070 (2010) [0912.0539 [hep-th]].

[11] C. F. Berger *et al.*, Phys. Rev. Lett. **102**, 222001 (2009) [0902.2760 [hep-ph]];
R. K. Ellis, K. Melnikov and G. Zanderighi, Phys. Rev. D **80**, 094002 (2009) [0906.1445 [hep-ph]];
C. F. Berger *et al.*, Phys. Rev. D **80**, 074036 (2009) [0907.1984 [hep-ph]];
G. Bevilacqua, M. Czakon, C. G. Papadopoulos and M. Worek, Phys. Rev. Lett. **104**, 162002 (2010) [1002.4009 [hep-ph]].

[12] Z. Bern, J. J. M. Carrasco, H. Johansson and D. A. Kosower, Phys. Rev. D **76**, 125020 (2007) [0705.1864 [hep-th]].

[13] Z. Bern, M. Czakon, D. A. Kosower, R. Roiban and V. A. Smirnov, Phys. Rev. Lett. **97**, 181601 (2006) [hep-th/0604074];
F. Cachazo, M. Spradlin and A. Volovich, Phys. Rev. D **78**, 105022 (2008) [0805.4832 [hep-th]];
M. Spradlin, A. Volovich and C. Wen, Phys. Rev. D **78**, 085025 (2008) [0808.1054 [hep-th]].

[14] Z. Bern, L. J. Dixon, D. A. Kosower, R. Roiban, M. Spradlin, C. Vergu and A. Volovich, Phys. Rev. D **78**, 045007 (2008) [0803.1465 [hep-th]];
C. Vergu, 0908.2394 [hep-th];
D. A. Kosower, R. Roiban and C. Vergu, 1009.1376 [hep-th].

[15] N. Arkani-Hamed, J. L. Bourjaily, F. Cachazo, S. Caron-Huot and J. Trnka, 1008.2958 [hep-th].

[16] Z. Bern, J. J. Carrasco, L. J. Dixon, H. Johansson, D. A. Kosower and R. Roiban, Phys. Rev. Lett. **98**, 161303 (2007) [hep-th/0702112].

[17] Z. Bern, J. J. M. Carrasco, L. J. Dixon, H. Johansson and R. Roiban, Phys. Rev. D **78**, 105019 (2008) [0808.4112 [hep-th]].

[18] Z. Bern, J. J. Carrasco, L. J. Dixon, H. Johansson and R. Roiban, Phys. Rev. Lett. **103**, 081301 (2009) [0905.2326 [hep-th]].

[19] Z. Bern, J. J. M. Carrasco and H. Johansson, 0902.3765 [hep-th];
L. J. Dixon, 1005.2703 [hep-th].

[20] Z. Bern, L. J. Dixon and D. A. Kosower, Nucl. Phys. B **513**, 3 (1998) [hep-ph/9708239].

[21] Z. Bern and A. G. Morgan, Nucl. Phys. B **467**, 479 (1996) [hep-ph/9511336].

[22] Z. Bern, L. J. Dixon, D. C. Dunbar and D. A. Kosower, Phys. Lett. B **394**, 105 (1997) [hep-th/9611127];
Z. Bern, L. J. Dixon and D. A. Kosower, JHEP **0001**, 027 (2000) [hep-ph/0001001].

[23] R. Britto, F. Cachazo and B. Feng, Nucl. Phys. B **725**, 275 (2005) [hep-th/0412103].

[24] E. I. Buchbinder and F. Cachazo, JHEP **0511**, 036 (2005) [[hep-th/05061xo26].

[25] R. Britto, B. Feng and P. Mastrolia, Phys. Rev. D **73**, 105004 (2006) [hep-ph/0602178];
C. Anastasiou, R. Britto, B. Feng, Z. Kunszt and P. Mastrolia, Phys. Lett. B **645**, 213 (2007) [hep-ph/0609191], JHEP **0703**, 111 (2007) [hep-ph/0612277].
P. Mastrolia, Phys. Lett. B **644**, 272 (2007) [hep-th/0611091];
R. Britto, B. Feng and G. Yang, JHEP **0809**, 089 (2008) [0803.3147 [hep-ph]].

[26] G. Ossola, C. G. Papadopoulos and R. Pittau, Nucl. Phys. B **763**, 147 (2007) [hep-ph/0609007].

[27] D. Forde, Phys. Rev. D **75**, 125019 (2007) [0704.1835 [hep-ph]].

[28] R. Britto and B. Feng, Phys. Rev. D **75**, 105006 (2007) [hep-ph/0612089];
W. B. Kilgore, 0711.5015 [hep-ph];
R. Britto, B. Feng and P. Mastrolia, Phys. Rev. D **78**, 025031 (2008) [0803.1989 [hep-ph]].

[29] F. Cachazo and D. Skinner, 0801.4574 [hep-th].

[30] W. T. Giele, Z. Kunszt and K. Melnikov, JHEP **0804**, 049 (2008) [0801.2237 [hep-ph]].

[31] S. D. Badger, JHEP **0901**, 049 (2009) [0806.4600 [hep-ph]].

[32] F. A. Berends, R. Kleiss, P. De Causmaecker, R. Gastmans and T. T. Wu, Phys. Lett. B **103**, 124 (1981);
P. De Causmaecker, R. Gastmans, W. Troost and T. T. Wu, Nucl. Phys. B **206**, 53 (1982);
Z. Xu, D. H. Zhang and L. Chang, TUTP-84/3-TSINGHUA;

R. Kleiss and W. J. Stirling, Nucl. Phys. B **262**, 235 (1985);
J. F. Gunion and Z. Kunszt, Phys. Lett. B **161**, 333 (1985);
Z. Xu, D. H. Zhang and L. Chang, Nucl. Phys. B **291**, 392 (1987).
[33] M. L. Mangano and S. J. Parke, Phys. Rept. **200**, 301 (1991);
L. J. Dixon, in *QCD & Beyond: Proceedings of TASI '95*, ed. D. E. Soper (World Scientific, 1996) [hep-ph/9601359].
[34] C. Cheung and D. O'Connell, JHEP **0907**, 075 (2009) [0902.0981 [hep-th]].
[35] V. P. Nair, Phys. Lett. B **214**, 215 (1988);
A. Brandhuber, P. Heslop and G. Travaglini, Phys. Rev. D **78**, 125005 (2008) [0807.4097 [hep-th]].
[36] J. M. Drummond, J. Henn, G. P. Korchemsky and E. Sokatchev, Nucl. Phys. B **828**, 317 (2010) [0807.1095 [hep-th]].
[37] M. Bianchi, H. Elvang and D. Z. Freedman, JHEP **0809**, 063 (2008) [0805.0757 [hep-th]];
J. M. Drummond, J. Henn, G. P. Korchemsky and E. Sokatchev, 0808.0491 [hep-th];
N. Arkani-Hamed, F. Cachazo and J. Kaplan, JHEP **1009**, 016 (2010) [0808.1446 [hep-th]];
H. Elvang, D. Z. Freedman and M. Kiermaier, JHEP **0904**, 009 (2009) [0808.1720 [hep-th]].
[38] Z. Bern, J. J. M. Carrasco, H. Ita, H. Johansson and R. Roiban, Phys. Rev. D **80**, 065029 (2009) [0903.5348 [hep-th]].
[39] Z. Bern *et al.*, 0803.0494 [hep-ph].
[40] C. F. Berger *et al.*, Phys. Rev. D **78**, 036003 (2008) [0803.4180 [hep-ph]].
[41] Z. Bern, L. J. Dixon and D. A. Kosower, Phys. Rev. D **73**, 065013 (2006) [hep-ph/0507005];
D. Forde and D. A. Kosower, Phys. Rev. D **73**, 061701 (2006) [hep-ph/0509358];
C. F. Berger, Z. Bern, L. J. Dixon, D. Forde and D. A. Kosower, Phys. Rev. D **74**, 036009 (2006) [hep-ph/0604195].
[42] Z. Bern, L. J. Dixon and D. A. Kosower, JHEP **0408**, 012 (2004) [hep-ph/0404293].
[43] T. Dennen, Y. t. Huang and W. Siegel, JHEP **1004**, 127 (2010) [0910.2688 [hep-th]].
[44] R. H. Boels, 0908.0738 [hep-th].
[45] R. H. Boels, 1008.3101 [hep-th].
[46] Z. Bern, J. S. Rozowsky and B. Yan, Phys. Lett. B **401**, 273 (1997) [hep-ph/9702424].
[47] Z. Bern, J. J. M. Carrasco, L. J. Dixon, H. Johansson and R. Roiban, 1008.3327 [hep-th].
[48] L. F. Alday, J. M. Henn, J. Plefka and T. Schuster, JHEP **1001**, 077 (2010) [0908.0684 [hep-th]];
J. M. Henn, S. G. Naculich, H. J. Schnitzer and M. Spradlin, JHEP **1004**, 038 (2010) [1001.1358 [hep-th]]; JHEP **1008**, 002 (2010) [1004.5381 [hep-th]].
[49] Z. Bern, L. J. Dixon, D. C. Dunbar, M. Perelstein and J. S. Rozowsky, Nucl. Phys. B **530**, 401 (1998) [hep-th/9802162].
[50] Z. Bern, J. J. M. Carrasco and H. Johansson, Phys. Rev. Lett. **105**, 061602 (2010) [1004.0476 [hep-th]].
[51] N. Arkani-Hamed and J. Kaplan, JHEP **0804**, 076 (2008) [0801.2385 [hep-th]].
[52] Z. Bern, T. Dennen, Y. t. Huang and M. Kiermaier, Phys. Rev. D **82**, 065003 (2010) [1004.0693 [hep-th]].
[53] L. M. Brown and R. P. Feynman, Phys. Rev. **85** (1952) 231;
L. M. Brown, Nuovo Cim. **21**, 3878 (1961);
G. Passarino and M. J. G. Veltman, Nucl. Phys. B **160**, 151 (1979);
Z. Bern, L. J. Dixon and D. A. Kosower, Nucl. Phys. B **412**, 751 (1994) [hep-ph/9306240].
[54] Z. Bern and D. A. Kosower, Nucl. Phys. B **379**, 451 (1992);
Z. Bern, A. De Freitas, L. J. Dixon and H. L. Wong, Phys. Rev. D **66**, 085002 (2002) [hep-ph/0202271].
[55] G. 't Hooft and M. J. G. Veltman, Nucl. Phys. B **44**, 189 (1972).
[56] Z. Bern, L. J. Dixon and D. A. Kosower, Phys. Rev. D **72**, 125003 (2005) [hep-ph/0505055].
[57] H. Kawai, D. C. Lewellen and S. H. H. Tye, Nucl. Phys. B **269**, 1 (1986);
Z. Bern, A. De Freitas and H. L. Wong, Phys. Rev. Lett. **84**, 3531 (2000) [hep-th/9912033];
Z. Bern, Living Rev. Rel. **5**, 5 (2002) [gr-qc/0206071];
N. E. J. Bjerrum-Bohr, P. H. Damgaard, B. Feng and T. Sondergaard, 1005.4367 [hep-th].
[58] Z. Bern, J. J. M Carrasco, L. Dixon and M. Douglas, in progress.
[59] T. Dennen and Y-t. Huang, in progress.
[60] D. A. Kosower, R. Roiban and C. Vergu, 1009.1376 [hep-th].
[61] S. Caron-Huot and D. O'Connell, to appear